[52] G. Güntherodt, J.L. Freeouf and F. Holtzberg, Phys. Rev., to be published.
[53] R. Evans, B.L. Gyorffy, N. Szabo and J.M. Ziman, in: Proc. Intern. Conf. Liquid Metals (1973) p. 319.
[54] G. Busch, P. Junod, P. Schwob, O. Vogt and F. Hulliger, Phys. Letters 9 (1964) 7.
[55] R.D. Parks, AIP Conf. Proc. 5 (1972) 630.
[56] D.D. Berkner, Phys. Letters 54A (1975) 396.
[57] W. Zinn, J. Magn. Matnet. Mater. 3 (1976) 23.
[58] O.W. Dietrich, A.J. Henderson Jr. and H. Meyer, Phys. Rev. B12 (1975) 2844.
[59] J.B. Goodenough, Magnetism and the Chemical Bond (Wiley, New York, 1963).
[60] T. Kasuya and A. Yanase, Rev. Mod. Phys. 40 (1968) 684.
[61] T. Kasuya, IBM Res. Developm. 14 (1970) 214.
[62] G. Busch, P. Junod, O. Vogt and F. Hulliger, Phys. Letters 6 (1963) 79.
[63] G. Busch, P. Schwob, O. Vogt and F. Hulliger, Phys. Letters 11 (1964) 100.
[64] A. Iandelli, in: Rare Earth Research, ed. E.V. Kleber (Macmillan, New York, 1961).
[65] J. Vitins and P. Wachter, Phys. Rev. B12 (1975) 3829.
[66] M.I. Darby and K.N.R. Taylor, Phys. Letters 14 (1965) 179.
[67] F. Holtzberg, T.R. McGuire, S. Methfessel and J.C. Suits, J. Appl. Phys. 35 (1964) 1033.
[68] T.R. McGuire and F. Holtzberg, AIP Conf. Proc. 5 (1971) 855.
[69] W. Beckenbaugh, G. Güntherodt, R. Hauger, E. Kaldis, J.P. Kopp and P. Wachter, AIP Conf. Proc. 18 (1974) 540.
[70] J. Feinleib and C.R. Pidgeon, Phys. Rev. Letters 23 (1959) 1391.
[71] M. Campagna, E. Kaldis and H.C. Siegmann, Helv. Phys. Acta 45 (1972) 4.
[72] J. Sakurai, Y. Kubo, T. Kondo, J. Pierre and E.F. Bertaut, J. Phys. Chem. Solids 34 (1973) 1305.
[73] K. Westerholt and S. Methfessel, in: Proc. Intern. Conf. Magnetism, Amsterdam, 1976, eds. P.F. de Châtil and J.J.M. Franse [Physica 86–88 B/C (1977) 1160].
[74] G. Busch, E. Kaldis, E. Schaufelberger-Teker and P. Wachter, in: Coll. Intern. du CNRS, No. 180, Les Elements des Terres Rares (1970) 359.
[75] P. Wachter, E. Kaldis and R. Hauger, to be published.

MUON PHYSICS

Florian SCHECK

Institut für Physik, Johannes Gutenberg-Universität, 6500 Mainz, Germany

NORTH-HOLLAND PUBLISHING COMPANY – AMSTERDAM

PHYSICS REPORTS (Review Section of Physics Letters) 44, No. 4 (1978) 187–248. North-Holland Publishing Company

MUON PHYSICS

Florian SCHECK

Institut für Physik, Johannes Gutenberg-Universität, 6500 Mainz, Germany

Received October 1977

Contents:

1. Introduction

The muon is known to us for a little more than forty years. It was discovered by Anderson and Neddermeyer [1] around 1936 in studies of cosmic rays with cloud chambers and Geiger counters. The mass of the muon was found to be around 200 to 240 times the mass of the electron and there were indications that there are positrons among the decay products of the positive muon [1c].

As is well known, for a long time the muon was believed to be identical with the meson which Yukawa had predicted to be responsible for the nuclear forces [2]. It was only in 1947 that the experiment of Conversi, Pancini and Piccioni [3] on the disintegration of negative muons in dense materials showed clearly that the muon was not absorbed through strong interaction and hence could not be Yukawa's π meson. Indeed, it was found that negative muons stopped in carbon have an appreciable chance of undergoing free decay rather than being captured by the nucleus. This was in contrast to calculations of muon capture which were based on the assumption that the muon had strong interaction and which predicted that there should essentially be no free decay even in carbon [4]. Actually, the question whether the muon has any "anomalous" interaction other than gravitational, weak and electromagnetic, has been accompanying muon physics like a cantus firmus throughout the last four decades. To give just one example, we mention the recent renewed interest in "anomalous" interactions of the muon that was raised by an apparent discrepancy of the radiative corrections in heavy muonic atoms (see section 4 below). A fair discussion of the situation is given in a paper by Okun and Zakharov [5] from which the earlier literature on the subject can be traced back easily. Today we formulate this question more precisely by asking whether there are any deviations from *muon–electron universality*, i.e. from the hypothesis that the muons (and their neutrinos) have exactly the same electromagnetic and weak couplings as electrons and electron neutrinos (see also section 2 below).

Quantitative and systematic investigations of muon interactions became possible only with the advent of muon beams from accelerators in the early 1950's. For instance, X-rays of muonic atoms (still with cosmic ray muons) had already been identified in 1949 by W.Y. Chang [6] but the results were only of qualitative nature. The first accelerator experiment by Fitch and Rainwater in 1953 [7] at once gave strong support to the assumption that the muon had mass about $210m_e$, that it had spin $\frac{1}{2}$ and that it had no anomalous interaction with the nucleus.

A similarly important cornerstone of muon physics was the experiment on $\pi^+ \to \mu^+ \to e^+$ decay carried out by Garwin, Lederman and Weinrich [8], and by Friedman and Telegdi [9]. It established at once that parity was not conserved in muon (and pion) decay, that the g-factor of the muon was 2 and that the spin of the positive muon was $\frac{1}{2}$. It was found, in particular, that muons from pion decay have a strong longitudinal polarization, and that the angular distribution of the decay electrons shows a large asymmetry with respect to the muon spin. These two facts are the basis of most experiments with muons which have been carried out since.

In parallel to these and many other investigations of the properties of the muon itself, many experiments have been carried out since the early 1950's in which the muon served as a *probe* in other domains of physics and other sciences. Indeed the muon has turned out to be a very useful test particle in nuclear physics, high-energy physics, solid state physics and chemistry.

The specific *spatial* properties of muonic atoms and their implications for the study of nuclear charge structure were discussed extensively by Wheeler [10] in 1949. The *time scale* of the muonic cascade was studied, among other important topics, in the classical paper by E. Fermi and E. Teller in 1947 [11] who showed that the whole cascade takes only about 10^{-13} to 10^{-14} seconds. How-

ever, the specific interplay of lifetimes of nuclear excited states, of muonic cascade times, and of the lifetime of the muon before it is captured (or decays freely), which is at the basis of so many beautiful applications in nuclear physics, was only fully realized and exploited in the mid-sixties (see section 5 below)*.

In modern high-energy physics the muon has become an important test particle in the investigation of both electromagnetic and weak interactions of hadronic particles. Its application started with the study of pion decay and of nuclear muon capture [13], and extends far into present-day investigations in the fields of electron–positron colliding beam physics and of neutrino physics at high energies.

The usefulness of the muon for solid state physics and chemistry was probably first realized in the classical work by Garwin, Lederman and Weinrich [8] from which we quote a sentence (p. 1416): "It seems possible that polarized positive and negative muons will become a powerful tool for exploring magnetic fields in nuclei, ..., atoms and interatomic regions". Studies of molecular and atomic states of negative muons, as well as of the precession of free positive muons and of muonium have been carried out occasionally since the early sixties, often as byproducts of experiments whose main goal lay in nuclear and particle physics. However since the high fluxes of the "meson factories" LAMPF, SIN and TRIUMF have become available recently, the fields of *Muonic chemistry* and *μSR* (*muon spin resonance*) as they are now being called, are receiving great attention in their own right and there is at present a wealth of data and unexpected phenomena awaiting theoretical analysis.

This review on *muon physics* is organized as follows. The present section 1 contains some introductory and historical remarks, as well as the usual excuses and apologies. In section 2 we summarize the basic properties of the muon and its neutrino, including a short résumé of possible lepton number schemes and of muon–electron universality. Section 3 which is perhaps the central part of this article deals with the weak interactions of the muon, i.e. discusses all its allowed and its (perhaps) forbidden decay modes, and its reactions with nucleons. Section 4 is devoted to electromagnetic properties of muons such as the magnetic moment, the g-factor and radiative corrections to bound muonic systems, as well as other topics. The final section 5 deals with the muon as a probe in particle and nuclear physics, stressing a few applications that seem particularly beautiful and instructive. A short appendix, finally, defines a few symbols that appear in the text and summarizes our notation.

We have tried to write this review in a somewhat pedagogical spirit with the hope that newcomers to the field of muon physics might find it useful for a first tour d'horizon. At the same time we try to work out a few topics that seem particularly interesting to us and where there is hope to make further progress in our understanding of the nature of the muon and its interactions. This implies in particular that this review cannot aim at completeness neither in the choice of topics nor in its reference to the literature. An article that gives a *complete* survey of a field as vast as muon physics, would necessarily come out somewhat dull and is not likely to inspire fresh enthusiasm for this domain of physics. Nevertheless we have made an effort to quote as many references as possible so that it should be easy to complete the literature on any particular subject by means of these key references. We apologize to all those whose important contributions to muon physics we do not quote explicitly. Readers who are interested in more details on specific subsections or

* We recall, however, that resonance phenomena between muonic transitions and excitations of deformed nuclei had been predicted by Wilets and by Jacobson in 1954 [12].

topics that are not dealth with in this article may also consult the three-volume monograph on "muon physics" edited by V. Hughes and C.S. Wu [14] (but should keep in mind that many articles of this book were completed around 1972 and may not be up-to-date in some respects).

There are some topics which we discuss only very briefly or which we have omitted deliberately. One of these is *nuclear muon capture* a detailed discussion of which we omit for two reasons. First, muon capture quickly leads more into a discussion of nucleonic weak interactions as well as nuclear structure aspects rather than of muon physics itself. Second, there already exists a recent and complete review on nuclear muon capture by N. Mukhopadhyay [15] which summarizes the literature up to June 1976 and to which we would have had little to add. Similarly, our remarks on applications of muons to solid state physics and chemistry are rather brief. On the one hand we do not feel competent enough to give a comprehensive introduction to μSR and muon chemistry; on the other hand these young fields are still in an exploratory stage and seem to need a lot more theoretical analysis. It might seem too early for a comprehensive summary at the present time*.

2. Basic properties of muons and their neutrinos

In this section we start with a résumé of the fundamental static properties of the muon and its neutrino (mass, charge, magnetic moment etc.) as well as their quantum number assignments. We then turn to a first short discussion of production and decay of muons. The third and last subsection deals with muon-electron universality and places the muon in the context of the lepton family.

Much of the material of this section is taken up in somewhat more detail in later sections, specifically sections 3 and 4 below.

2.1. Static properties and quantum numbers

2.1.1. The muon (μ^-) and its antiparticle (μ^+)

The charge of the muon is known to be equal to the charge of the electron within about 2 ppm. The best and most recent determination of the muon to electron *mass ratio* gives the result [17]

$$m_\mu/m_e = 206.76859\,(29) \quad (1.4\ \text{ppm}). \tag{2.1}$$

The electron mass m_e as quoted in the review of particle properties [18] is known to 2.7 ppm, giving

$$m_\mu = 105.65945\,(32)\ \text{MeV}/c^2 \quad (3\ \text{ppm}). \tag{2.2}$$

The charge and the mass ratio (2.1) are obtained by combining measured values of (i) the magnetic moment ratio μ_μ/μ_p; (ii) the hyperfine splitting of muonium $\Delta\nu_0$; and (iii) the anomaly of the muon's g-factor $a \equiv \frac{1}{2}(g_\mu - 2)$. To understand this we recall that $\Delta\nu_0$ in lowest approximation is given by Fermi's contact interaction

$$\Delta\nu_0 \simeq -\frac{32}{3}\mu_\mu\mu_e \frac{1}{a_B^3}\frac{1}{h} \tag{2.3}$$

* An account of μSR experimental possibilities is found in the article by Brewer et al. in Vol. II of ref. [14] and in [16].

where $\mu_i = \frac{1}{2} g_i e_i / 2m_i$ denotes the magnetic moment, g_i the g-factor, and where $a_B = (m_e + m_\mu)/(e_\mu e_e \cdot m_e m_\mu)$ is the Bohr radius. (This formula is very rough and is used here for illustrational purposes only. For details see section 4.2.1.) Thus

$$\Delta\nu_0 \simeq \frac{16}{3} R_\infty \alpha^2 c \left(\frac{g_\mu}{2}\right)\left(\frac{g_e}{2}\right)\left(\frac{m_e}{m_\mu}\right)\left(\frac{e_\mu}{e_e}\right)^4 \left(1 + \frac{m_e}{m_\mu}\right)^{-3}, \qquad R_\infty = m_e c\alpha^2/2h \tag{2.4}$$

where R_∞ is the Rydberg constant and where α is defined in terms of e_e, $\alpha = e_e^2/\hbar c$.

Furthermore

$$\frac{m_\mu}{m_e} = \frac{\mu_p}{\mu_\mu}\frac{\mu_e}{\mu_p}\frac{|g_\mu|}{|g_e|} \tag{2.5}$$

where μ_p is the magnetic moment of the proton. Eq. (2.5) is utilized in determining the mass ratio, while e_μ/e_e can be obtained from eq. (2.4).

The *spin* of the muon is $\frac{1}{2}$. This follows from the observed fine structure of bound μ^- systems (muonic atoms) and of muonium ($\mu^+ e^-$). Therefore the muon is a fermion, μ^+ and μ^- have opposite intrinsic parity.

The *magnetic moment* of the muon can be obtained either through a direct measurement of the precession of the muon spin in a known magnetic field or from a combination of muonium transition frequencies in strong magnetic fields (see below, section 4). Since magnetic field strengths are determined through proton spin resonance it is the ratio μ_μ/μ_p that is determined. The most recent value is

$$\mu_\mu/\mu_p = 3.1833417(39) \qquad (1.2 \text{ ppm}). \tag{2.6}$$

This is the weighted average of a measurement in muonium [17] and of a spin precession experiment in liquids [19]. Finally we quote the most recent value of the *g-factor anomaly* (to which we also return in section 4)

$$a_\mu \equiv \tfrac{1}{2}(g_\mu - 2) \tag{2.7}$$

as obtained in the latest CERN experiment with the Muon Storage Ring [20]:

$$a_{\mu^+} = 1165910(12) \times 10^{-9} \qquad (10 \text{ ppm}) \tag{2.8}$$

$$a_{\mu^-} = 1165936(12) \times 10^{-9} \qquad (10 \text{ ppm}) \tag{2.9}$$

which combine to the weighted average value

$$a_\mu = 1165922(9) \times 10^{-9} \qquad (8 \text{ ppm}). \tag{2.10}$$

Finally, we comment on a possible *electric dipole moment* of the muon. If muon interactions are invariant under time reversal the static electric dipole moment d_μ is zero. The present experimental limit is [20]

$$d_\mu < 8 \times 10^{-19}\, e\,\text{cm}. \tag{2.11}$$

2.1.2. The muon neutrino

The knowledge of the static properties of the muon neutrino ν_μ and its antiparticle $\bar{\nu}_\mu$ is considerably poorer than for the muon itself. To date the best limit on the *mass* in a direct measurement is obtained from Kμ3 decay [21]

$$m_{\nu_\mu} < 0.65 \text{ MeV}/c^2. \tag{2.12}$$

Further direct experiments to measure m_{ν_μ} from pion decay in flight are in progress at SIN [22] but will eventually improve the limit (2.12) only to about 0.2 MeV/c^2. An *indirect* determination of m_{ν_μ} can be obtained from a measurement of the momentum q of the decay muon from pions at rest, and using the muon and pion masses as input [23]

$$m_{\nu_\mu}^2 = (m_\pi^2 + m_\mu^2) - 2m_\pi\sqrt{q^2 + m_\mu^2}.$$

The latest (still preliminary) value of q is [23e]

$$q = (29.7886 \pm 0.0017) \text{ MeV}/c. \tag{2.13}$$

This gives a value for m_{ν_μ} that is compatible with zero but the error is large, of the order of $\Delta m_{\nu_\mu}^2 = 0.19 \text{ MeV}^2/c^4$. The main limitation is the uncertainty in the pion mass which is still of the order of 5×10^{-5}. Also, the pion mass, when taken from transition energies of pionic atoms, depends on the theoretical understanding of these atomic spectra. Thus, a direct and precise measurement of the pion mass as proposed for example in [22] would be of great utility in this context.

Nevertheless a really novel idea is still lacking as to how m_{ν_μ} could be bounded to a similar precision as the mass of the electronic neutrino (about 60 eV, see [18]) through a direct measurement*. Obviously, it is of utmost importance for our understanding of the leptons to establish the masslessness of the muonic neutrino.

The neutrinos are electrically neutral and have no magnetic moment. The evidence for this comes from astrophysical arguments [24]. Indeed if the neutrinos had electromagnetic attributes such as charge, charge radius, or magnetic dipole moment, a plasmon in the sun could decay electromagnetically into neutrino–antineutrino pairs. The known lifetime of the sun ($> 5 \times 10^9$ y) puts rather strong limits on these quantities:

$$e_\nu/e < 10^{-13}; \qquad \langle r^2 \rangle < 10^{-27}\,\text{cm}^2 \tag{2.14}$$

$$\mu_\nu \Big/ \left(\frac{e}{2mc}\right) < 10^{-10}. \tag{2.15}$$

Actually, these limits hold primarily for the electron neutrino; they are also applicable to the muon neutrino provided its mass is below 1 keV [25].

There is good evidence from pion and muon decays that ν_μ is left-handed (negative helicity) and that $\bar{\nu}_\mu$ is right-handed (positive helicity) – although it is not clear to which precision this is known experimentally. The first experiments which confirmed this assignment directly by measuring the polarization of the decay muon in $\pi \to \mu\nu_\mu$ were published in 1961 [26].

2.1.3. Lepton number assignments

Not much is known about the identification of the neutrinos in those leptonic and semi-leptonic weak interaction processes that are accessible in experiments. It is known that the neutrinos from $\pi^+ \to \mu^+\nu_\mu$ decay do not induce inverse beta decay, i.e. [27]

$$\nu_\mu + (Z, A) \nrightarrow (Z + 1, A) + e^-$$

* An analysis of the decay $\pi \to \mu\nu_\mu\gamma$ at the upper end of the photon spectrum, whose form depends on the neutrino mass, has been discussed off and on at the "meson factories" but this seems an impossible task in view of background problems.

where (Z, A) denotes a nucleus with charge number Z and mass number A. It is known that decays like $\mu \to e\gamma$ ($\mu \to e\bar{e}e$) are absent to a level of less than one in $10^8(10^9)$ muon decays (see section 3.5 below). The values $\rho = \frac{3}{4}$, $\xi = 1$ of the decay parameters in ordinary muon decay $\mu \to e\nu_1\bar{\nu}_2$, together with the polarization of the decay electron, imply that ν_1 and $\bar{\nu}_2$ have opposite helicity. However, a clear identification of these particles has not been possible yet. The following scheme is *compatible* with all available observations. One should keep in mind, however, that it is by no means well established experimentally and therefore should be considered as a working hypothesis that may possibly have to be modified later on.

It is believed that muons and muon neutrinos carry a new quantum number L_μ which is zero for electrons and their neutrinos but is non-zero for μ, ν_μ and takes on the eigenvalues as indicated in table 2.1. Like the common lepton number L, the muon number L_μ is believed to be an *additive* constant of the motion in all electromagnetic as well as in all leptonic and semileptonic weak processes,

$$\sum_i L^{(i)} = \text{const.}, \qquad \sum_i L_\mu^{(i)} = \text{const.} \tag{2.16}$$

An alternative that also seems compatible with experiment is that muon lepton number is conserved in a *multiplicative* pattern [28] (while L is still additive), i.e.

$$\sum_i L^{(i)} = \text{const.}, \qquad (-)^{\sum_i L_\mu^i} = \text{const.} \tag{2.17}$$

For example in the *additive* scheme (2.16) μ^+-decay would proceed solely according to

$$\mu^+ \to e^+ + \nu_e + \bar{\nu}_\mu. \tag{2.18a}$$

In the *multiplicative* scheme both (2.18a) and the decay mode

$$\mu^+ \to e^+ + \bar{\nu}_e + \nu_\mu \tag{2.18b}$$

are possible, the branching ratio depending on the appropriate coupling constants in the interaction Hamiltonian. The mode (2.18b) could be detected by means of inverse β-decay induced by the $\bar{\nu}_e$ in ordinary matter

$$\bar{\nu}_e + p \to n + e^+.$$

This is again an experiment which is being considered at the new high-flux accelerators at intermediate energies. So far, a bubble chamber experiment at CERN gave the limit [29]

$$\Gamma(\mu^+ \to e^+\bar{\nu}_e\nu_\mu)/\Gamma(\mu^+ \to e^+\nu_e\bar{\nu}_\mu) < 0.25 \qquad \text{(at 90\% confidence level)}. \tag{2.19}$$

Finally, there is the scheme proposed long ago by Konopinski and Mahmoud [30] which introduces only one kind of additive lepton number L_{KM} but with the assignment

$$L_{KM}(e^-, \mu^+, \nu_e, \bar{\nu}_\mu) = +1, \qquad L_{KM}(e^+, \mu^-, \bar{\nu}_e, \nu_\mu) = -1 \tag{2.20}$$

with

$$\sum L_{KM} = \text{const.} \tag{2.21}$$

Unlike the other schemes this scheme requires electronic and muonic neutrinos to have the same mass. The KM scheme is compatible with all observations (but forbids the mode (2.18b)), and accomodates new processes which are forbidden in the other schemes. An example is neutrinoless μ^- capture with double charge exchange

$$\mu^- + (Z, A) \to (Z - 2, A) + e^+ \tag{2.22}$$

which we discuss below (section 3.5).

Table 2.1
Lepton number assignments in the additive scheme

Particle	e^-	ν_e	e^+	$\bar{\nu}_e$	μ^-	ν_μ	μ^+	$\bar{\nu}_\mu$
L	1	1	−1	−1	1	1	−1	−1
L_μ	0	0	0	0	1	1	−1	−1
Helicity		−1	+1			−1		+1

2.2. Production and decay of muons

2.2.1. Electromagnetic and weak production

Muons can be produced *electromagnetically* for instance in electron–positron collisions

$$e^+ + e^- \to \mu^+ + \mu^-. \tag{2.23}$$

This is a standard reaction in electron–positron physics which is used as a test of quantum electrodynamics at high energies and serves as a reference reaction for studies of electron–positron annihilation into hadrons*. The differential cross section in the center-of-mass (c.m.) system is given by

$$\frac{d\sigma_{\mu\mu}}{d\Omega} = \frac{\alpha^2}{4s}\beta\{(1 + \cos^2\theta) + (1 - \beta^2)\sin^2\theta\} \tag{2.24}$$

where s is the square of the c.m. energy, θ the scattering angle and $\beta = |\boldsymbol{p}_\mu|/E_\mu$, the ratio of muon three-momentum to muon energy in the c.m. system. The total cross section reads

$$\sigma_{\mu\mu} = \frac{4\pi\alpha^2}{3s}\left\{1 + \frac{1 - \beta^2}{2}\right\}\beta. \tag{2.25}$$

Its magnitude is $4\pi\alpha^2/3s \simeq 21.7 \times 10^{-33}\,\text{cm}^2$ for 1 GeV colliding beam energy.

Muon beams at accelerators are obtained from the *weak decay* of charged pions

$$\pi^\pm \to \mu^\pm + \nu_\mu(\bar{\nu}_\mu) \tag{2.26}$$

whose main characteristics are summarized here for reference purposes.

Due to conservation of angular momentum, and with the helicities of the neutrinos as given in table 2.1, the μ^+ from π^+ decay is polarized along the *negative* direction of its momentum, whilst the μ^- from π^- decay is polarized along the *positive* direction of its momentum. This holds in the system of reference in which the pion is at rest, and is illustrated in fig. 2.1, for the case of π^+ decay.

Let $\boldsymbol{q}^*$ be the momentum of the μ^+ in the c.m. system, $q^* = |\boldsymbol{q}^*|$ its magnitude and θ^* the angle that $\boldsymbol{q}^*$ makes with the direction of the pion momentum $\boldsymbol{p}_\pi$ in the laboratory frame. The cor-

* A summary of the experimental situation can be found in ref. [31].

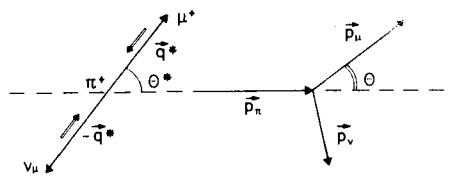

Fig. 2.1. Kinematic variables for $\pi \to \mu\nu_\mu$ decay in the pion rest system (left part) and in the laboratory system (right-hand part).

responding quantities in the laboratory system shall be denoted by $\boldsymbol{p}_\mu$, $p_\mu = |\boldsymbol{p}_\mu|$ and θ, respectively. Then the longitudinal polarization of the μ^+ in the *c.m. system* is*

$$P_l^* = \zeta^* \boldsymbol{q}^*/q^* = -1 \tag{2.27}$$

while in the *laboratory system* it is

$$P_l = -\frac{E_\pi\, q^*}{m_\pi\, p_\mu}\left\{1 + \beta_\pi \frac{E_\mu^*}{q^*}\cos\theta^*\right\}. \tag{2.28}$$

An alternative expression for this latter quantity is

$$P_l \doteq -\left\{\frac{E_\mu E_\mu^*}{p_\mu q} - \gamma_\pi \frac{m_\mu^2}{p_\mu q^*}\right\}. \tag{2.29}$$

Here, the quantities marked with an asterisk refer to the c.m., the quantities without asterisk refer to the laboratory system. Specifically, $q^* = (m_\pi^2 - m_\mu^2)/2m_\pi$, $E_\mu^* = m_\mu - q^* = (m_\pi^2 + m_\mu^2)/2m_\pi$, $\beta_\pi = |\boldsymbol{p}_\pi|/E_\pi$; $\gamma_\pi = E_\pi/m_\pi = (1 - \beta_\pi^2)^{-1/2}$.

These relations are derived by means of the covariant spin operator

$$s = \left(\frac{1}{m}\boldsymbol{p}\cdot\zeta; \zeta + \frac{\boldsymbol{p}\cdot\zeta}{m(E+m)}\boldsymbol{p}\right)$$

where ζ gives the spin direction and degree of polarization in the rest system of the particle. Further, the kinematic relationship

$$E_\mu = \gamma_\pi E_\mu^* + q^*\sqrt{\gamma_\pi^2 - 1}\cos\theta^* \tag{2.30}$$

has been used.

For emission in the forward or backward direction, $\theta^* = 0$ or π, one has the kinematic relation

$$\gamma_\pi = \frac{1}{m_\mu^2}\{E_\mu E_\mu^* \pm p_\mu q^*\}$$

(positive sign for $\theta^* = 0$, negative sign for $\theta^* = \pi$) and, therefore from eq. (2.29)

$$P_l(\theta^* = 0) = -1; \qquad P_l(\theta^* = \pi) = +1.$$

* For $\pi^- \to \mu^-$ decay P_l^* and P_l change sign.

P_l vanishes for muons emitted at an angle that satisfies*

$$\cos\theta^* = -q^*/\beta_\pi E_\mu^*$$

for which $\gamma_\pi = E_\mu E_\mu^*/m_\mu^2$.

In practice, if the energy spectrum of the pion beam is known and if the angular acceptance of the muon beam is given, the effective longitudinal polarization of the muon beam is obtained by integration over that energy spectrum and that angular range. In this way a partially polarized muon beam is obtained with polarizations of the order of 80% to 90% for cases of practical interest.

2.2.2. *Decay of muons*

The lifetime of the muon is known very accurately [18, 32],

$$\tau_\mu = 2.197134\,(77) \times 10^{-6}\ \text{sec}. \tag{2.31}$$

This lifetime is determined practically exclusively by the decay mode

$$\mu \to e + \nu + \bar{\nu} \tag{2.32}$$

and is the source for the determination of G, the Fermi coupling constant. The relation is (see eqs. (3.31) and (3.50) in section 3 below)

$$\frac{1}{\tau_\mu} = \frac{G^2 m_\mu^5}{192\pi^3}\left\{1 - 8\left(\frac{m_e}{m_\mu}\right)^2 + \frac{\alpha}{2\pi}\left(\frac{25}{4} - \pi^2\right) + O\left(\left(\frac{m_e}{m_\mu}\right)^3\right) + O(\alpha^2)\right\}. \tag{2.33}$$

The only other decay mode, muon radiative decay,

$$\mu \to e + \nu + \bar{\nu} + \gamma \tag{2.34}$$

that has been seen experimentally, has a branching ratio of less than 10^{-4}.**

Recent searches for a possible two-body decay into a new particle (scalar or pseudoscalar boson) x^+ and a neutrino,

$$\mu^+ \to x^+ + \overline{\nu_\mu} \tag{2.35}$$

have not seen such a decay mode [33]. For masses of the hypothetical x-particle between 60 MeV/c^2 and 85 MeV/c^2 and by assuming its lifetime to be longer than 200 μs, an upper limit of 2×10^{-6} for the branching ratio is quoted (at 90% c.l.). If the x particle decays into e^+ and ν_e, and if some model assumptions about this decay are made, this limit is lowered by about two orders of magnitude by the non-observation of such positrons.

Decay modes which violate the lepton number schemes mentioned above, are discussed below in section 3.5.

Although ordinary muon decay (2.32) is discussed in more detail below, sections 3.1–3.3, we summarize here its main characteristics. In the system of reference where the muon is at rest the differential decay probability with emission of the electron with energy E and with momentum $\boldsymbol{p}$ in a direction θ with respect to the muon spin is given by (see eq. (3.30d) below)

$$d\Gamma(x,\theta) \simeq \frac{1}{\tau_\mu}\{(3 - 2x) \mp P(2x - 1)\cos\theta\}x^2\,dx\,d(\cos\theta) \tag{2.36}$$

* Such an angle exists only for $\beta_\pi > 1 - 2m_\mu^2/(m_\pi^2 + m_\mu^2) \simeq 0.27$.

** This decay mode is discussed below, in section 3.4.

where $x = 2E/m_\mu$ is the reduced energy (electron energy divided by its maximal value $W \simeq m_\mu/2$) whose range is $0 \leqslant x \leqslant 1$ and where P is the muon polarization. The minus sign holds for $\mu^- \to e^-$ decay, the plus sign for $\mu^+ \to e^+$ decay. (The neutrino momenta have been integrated over.) The *average* asymmetry of the decay electrons, if their energy is not recorded, is obtained from eq. (2.36) upon integration over x from 0 to 1,

$$d\bar{\Gamma}(\theta) \simeq \frac{1}{2\tau_\mu}(1 \mp P\tfrac{1}{3}\cos\theta)d(\cos\theta). \tag{2.37}$$

This is the asymmetry that is observed if the muon spin precesses about a magnetic field and if the energy of the electron (positron) is not discriminated. From eq. (2.36) it is seen that *maximal* asymmetry is obtained for maximum energy, $x = 1$. The asymmetry vanishes, on the other hand at $x = \frac{1}{2}$. It is equal to its average value $\frac{1}{3}$ at $x = \frac{3}{4}$.

2.3. Muon–electron universality and the lepton family

2.3.1. Muon–electron universality, definition and tests

One of the most striking observations in the physics of muons, electrons and muonic and electronic neutrinos is the apparent universality of their interactions. The coupling of the muon to the photon field is exactly the same as the coupling of the electron to the photon field. One merely has to replace the electron field operator $\psi_e(x)$ by the muon field operator $\psi_\mu(x)$ and the physical electron mass m_e by the muon mass m_μ in the Hamiltonian of quantum electrodynamics. All QED processes involving muons are then calculable by means of the standard Feynman rules and depend only on α, the fine structure constant, on the electron mass and on the muon mass. Quantitative differences between electromagnetic observables of muons and the corresponding observables of electrons are due solely to the different masses of these particles.

There are many direct and indirect tests of electromagnetic muon–electron universality, both at low and high energies, some of which are discussed in section 4 below.

At low energies the most precise test case is the g-factor of the muon. Indeed, it is found that the muon g-factor anomaly is predicted correctly *up to the natural limit of QED*, i.e. up to the order where contributions from strong and weak interactions become significant (see section 4.1 below).

Although less precise to date, radiative corrections to bound muonic systems (muonium, muonic atoms, $\mu^-\pi^+$ etc.) are of no less interest due to the fact that these effects are complementary, to a large extent, to the Lamb shift in ordinary electronic atoms. Whilst the *electronic* Lamb shift is dominated by vertex correction and anomalous magnetic moment, radiative corrections to *muonic* bound states are dominated by vacuum polarization due to electron–positron pairs (see sections 4.2 and 4.3).

Tests of electromagnetic muon–electron universality at high energies are much less precise for experimental reasons and are mostly somewhat indirect. There are purely leptonic processes such as μ-pair production, eq. (2.23). There is also elastic as well as deep-inelastic scattering of muons on protons that can be compared to the corresponding processes with electrons.*

Muon–electron universality in *weak interactions* means that all weak interaction processes involving muons are described by the usual Hamiltonian for weak interactions merely by adding to the electronic weak currents the corresponding muonic weak currents with the electron and

* Summaries of the experimental situations can be found in the proceedings of recent conferences on high-energy physics and of the biennial topical conferences on photon and electron interactions at high energies.

electronic neutrino field operators $\psi_e(x)$, $\psi_{\nu_e}(x)$ replaced by the muon and muonic neutrino field operators $\psi_\mu(x)$, $\psi_{\nu_\mu}(x)$, respectively. For interactions involving charged currents, in particular, this means the replacement

$$\mathcal{L}_e^\alpha = \overline{\psi_e(x)}\gamma^\alpha(1-\gamma_5)\psi_{\nu_e}(x) \to \mathcal{L}^\alpha = \overline{\psi}_e\gamma^\alpha(1-\gamma_5)\psi_{\nu_e} + \overline{\psi}_\mu\gamma^\alpha(1-\gamma_5)\psi_{\nu_\mu}. \tag{2.38}$$

Here again, the coupling is universal. All quantitative differences between weak processes of electrons and muons are due to the difference in mass.

A rather precise test of muon–electron universality is provided by the branching ratio of charged pion decay into electron and electronic neutrino to the decay into muon and muonic neutrino,

$$R(e/\mu) = \Gamma(\pi \to e\nu_e)/\Gamma(\pi \to \mu\nu_\mu). \tag{2.39}$$

If semileptonic weak interactions are universal, then this ratio should depend only on the masses of these particles but the Fermi coupling constant G and the hadronic matrix element $\langle 0|\, h^\alpha\, |\pi^\pm\rangle$ should drop out. One finds indeed,

$$R_{th}^{(0)}(e/\mu) = \frac{m_e^2}{m_\mu^2}\left(\frac{1-(m_e/m_\pi)^2}{1-(m_\mu/m_\pi)^2}\right)^2. \tag{2.40}$$

To this one must still add the radiative corrections [34], giving the final numerical prediction*

$$R_{th}(e/\mu) = 1.233 \times 10^{-4}. \tag{2.41}$$

The most precise measurement of this branching ratio is the one published by Di Capua et al. [35a]. If corrected for the latest value of the pion lifetime [35b] their result is

$$R_{exp}(e/\mu) = (1.274 \pm 0.024) \times 10^{-4} \tag{2.42}$$

which agrees with the theoretical value within two standard deviations.

There are many more tests of muon–electron universality in weak interactions some of which are less direct than the example quoted above. For instance, the analysis of all semileptonic processes involving muons and muon neutrinos is always based on the universality hypothesis. Some of them can be compared directly to the corresponding electronic processes, some of them cannot (for experimental reasons). It is then the set of all observations that must be taken as test of the assumption of muon–electron universality.

As in the example (2.39) above, the predictions in lowest order are simple functions of the masses and kinematic variables involved. Depending on the experimental accuracy it may be necessary to take into account higher order weak and electromagnetic corrections. With the advent of renormalizable gauge theories these corrections have become calculable in a unique way starting from an interaction Hamiltonian that has muon–electron universality built in from the start. For a review on this topic and many references to original work see [36]**.

2.3.2. The lepton family

It would be beautiful if we could close this section by giving some simple classification scheme for the leptons that would provide us with a convincing insight into the role of their quantum

* These corrections depend on an ultraviolet cut-off Λ. If this is taken to be the same in $\pi \to e\nu$ and $\pi \to \mu\nu$ decay then the number in eq. (2.41) results. If $\Lambda(\pi \to e\nu)/\Lambda(\pi \to \mu\nu) = m_e/m_\mu$ is taken then $R_{th} = 1.258 \times 10^{-4}$. See discussion in [35b].

** Unfortunately there are not enough purely leptonic processes that can be studied in the laboratory so as to allow for a test of (leptonic) gauge theories by means of the higher-order corrections that they predict.

numbers. Unfortunately we are not able to do so as we know nothing about the nature and origin of the muonic lepton number. We have learnt to live with the four leptons

$$e, \nu_e, \mu, \nu_\mu$$

with (empirical) quantum numbers as given in table 2.1 and with universal weak and electromagnetic couplings as described above. The symmetry between these four leptons and the four types of quarks (three quarks corresponding to the triplet representation of SU(3), plus one charmed quark) that are at the basis of hadronic structure, is a very tempting idea. Many theoretical models that aim at unifying strong, electromagnetic and weak interactions do indeed exploit this apparent symmetry.

Recently evidence for the pair production of heavy leptons in electron–positron collisions,

$$e^+ + e^- \to L^+ + L^- \tag{2.43}$$

from μe events in the final state has been reported from SLAC and from DESY [37, 38]. If the interpretation is correct this particle has mass around 1.8 to 1.9 GeV/c^2. It is probably accompanied by its own neutrino and may decay into leptons,

$$L^\pm \to \mu^\pm \nu_\mu \nu_L, \qquad L^\pm \to e^\pm \nu_e \nu_L$$

but semileptonic decays into hadrons

$$L \to \nu_L + \text{hadrons}$$

should be important.

If the existence of this heavy lepton is confirmed, and if it indeed introduces a new conserved lepton number into lepton physics, this would obviously disturb the simple picture of a unified theory based on a four leptons–four quarks symmetry.

3. Weak interactions of muons and their neutrinos

In this section we review ordinary muon decay $\mu \to e\nu\bar{\nu}$ in some detail. We also discuss briefly muon radiative decay $\mu \to e\nu\bar{\nu}\gamma$ and related rare decay modes. The remaining part of the section is devoted to a discussion of muon lepton number and its tests in ultrarare muon decays and muon–electron conversion on nuclei.

3.1. Muon decay $\mu \to e\nu\bar{\nu}$

The principal decay mode of the muon

$$\mu^- \to e^- + \bar{\nu}_e + \nu_\mu \tag{3.1}$$

and its image under charge conjugation C

$$\mu^+ \to e^+ + \nu_e + \bar{\nu}_\mu \tag{3.2}$$

is still the most precise source of information on purely leptonic weak interactions. For this reason, and also because some of the pertinent formulae are not readily found in the literature, we wish to go into some detail. In particular, we review the present state of knowledge on the characteristics of this decay and point out what remains to be done.

The kinematical range of the electron spectrum is

$$\mu \leqslant E_e \leqslant W \equiv (m^2 + \mu^2)/2m. \tag{3.3}$$

In terms of the standard reduced energy variable

$$x \equiv E_e/W \tag{3.4a}$$

with $W = 52.831$ MeV we have

$$x_0 \leqslant x \leqslant 1. \tag{3.5}$$

Here m is the muon mass, μ is the electron mass, and

$$x_0 = \mu/W = 9.67 \times 10^{-3}. \tag{3.4b}$$

In this range of energies a four-fermion contact interaction of vector and axial vector type is practically indistinguishable from an interaction mediated by heavy vector bosons (with the same vector and-axial vector couplings to leptons) provided their mass is greater than, say, about 10 GeV. It is justified, therefore, to discuss muon decay in terms of the contact interaction only. The modifications due to the finite mass of possible intermediate vector bosons are discussed at the end of this section.

To date only measurements on the decay electron can be performed and no direct measurement on the neutrinos is feasible. Information on the decay must therefore be extracted from decay characteristics of the electron, such as energy spectrum, spin-momentum correlations and spin–spin correlations. Therefore, in confirming the "V-A" interaction, the best one can hope to obtain eventually is the effective leptonic Hamiltonian density

$$\mathscr{H}_{\text{leptonic}} = \frac{G}{\sqrt{2}}[\bar{e}\gamma^a(1 - \gamma_5)\mu][\bar{\nu}_\mu\gamma_a(1 - \lambda\gamma_5)\nu_e] + \text{h.c.} \tag{3.6}$$

The parameter λ remains undetermined as long as no direct measurement on the neutrinos is available. Unfortunately, our present experimental information is not sufficient for confirming the interaction (3.6). The data on muon decay are still compatible with rather large deviations from pure "V-A".

In this section we review the definition of the decay parameters, discuss their experimental values and point out what remains to be done, before we can be sure that the interaction is really the one of eq. (3.6).

For that purpose we write down the decay probability for the most general four-fermion interaction, reducing it then to the simplified form that corresponds to the "V-A" case.

The differential decay probability for an electron with energy between x and $x + dx$, emitted at an angle between θ and $\theta + d\theta$ with respect to the muon spin direction, and having its spin pointing in the direction (ϕ, ψ) (see fig. 3.1) is given by

$$\frac{d^2\Gamma^{(0)}(x, \theta, \phi, \psi)}{dx\, d(\cos\theta)} = \frac{mW^4A}{32\pi^3}\sqrt{x^2 - x_0^2}\left\{[x(1 - x) + \tfrac{2}{9}\rho(4x^2 - 3x - x_0^2) + \eta x_0(1 - x)]\right.$$
$$\left. - \tfrac{1}{3}\xi\sqrt{x^2 - x_0^2}\cos\theta\left[1 - x + \tfrac{2}{3}\delta\left(4x - 3 - \frac{\mu}{m}x_0\right)\right] + \right.$$

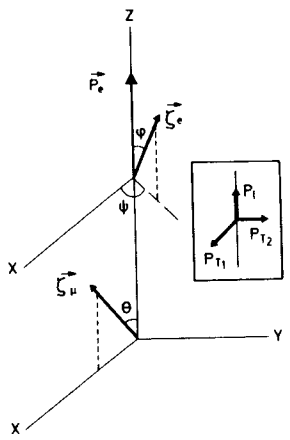

Fig. 3.1. Kinematic variables for the decay $\mu \to e\nu\bar{\nu}$ in the muon rest system. ζ_μ: spin direction of muon; ζ_e, p_e: spin direction and three-momentum of electron, respectively. The inserted figure defines the three components of the electron polarization vector (see text).

$$
\begin{aligned}
&- \xi' \sqrt{x^2 - x_0^2} \cos\phi \left[1 - x + \tfrac{2}{3}\delta' \left(4x - 3 - \frac{\mu}{m} x_0 \right) \right] \\
&+ \tfrac{1}{3}\xi'' \cos\theta \cos\phi \left[x(1-x) + \tfrac{2}{3}\rho'(4x^2 - 3x - x_0^2) + \eta' x_0 (1-x) \right] \\
&+ \sin\theta \sin\phi \cos\psi \left[(1-x) x_0 \frac{3a - 2b - 2c}{3A} + x(1-x)\frac{\alpha}{A} + (x - x_0^2)\frac{2\beta}{3A} \right] \\
&+ \sin\theta \sin\phi \sin\psi \sqrt{x^2 - x_0^2} \left[(1-x)\frac{\alpha'}{A} + \tfrac{2}{3}\left(1 - \frac{\mu}{m} x_0 \right)\frac{\beta'}{A} \right] \Bigg\}. \qquad (3.7)
\end{aligned}
$$

The kinematical variables x, θ, ϕ, and ψ are defined in eq. (3.4) and in fig. 3.1, respectively. The parameters $\rho, \eta, \ldots \beta'$ which enter this lengthy expression are defined in terms of bilinear combinations of the coupling constants of the general four fermion interaction. In view of the fact that so far we can determine only the $\bar{e} \ldots \mu$ piece of eq. (3.6) it is natural to start from the interaction written in the charge retention form

$$
\mathcal{H} = \sum_i \{ C_i (\overline{e(x)} \Gamma_i \mu(x)) (\overline{\nu_\mu(x)} \Gamma^i \nu_e(x)) + C_i' (\overline{e(x)} \Gamma_i \mu(x)) (\overline{\nu_\mu(x)} \Gamma^i \gamma_5 \nu_e(x)) + \text{h.c.} \} \qquad (3.8)
$$

where Γ_i stands for the scalar, vector, axial vector, pseudoscalar and tensor operators, respectively,

$$
\Gamma_S = \mathbf{1}, \qquad \Gamma_V = \gamma^\mu, \qquad \Gamma_A = \gamma^\mu \gamma_5, \qquad \Gamma_P = i\gamma_5, \qquad \Gamma_T = \frac{1}{\sqrt{2}} \sigma^{\mu\nu}. \qquad (3.9)
$$

Defining, as usual, the following real quantities

$$
a = |C_S|^2 + |C_S'|^2 + |C_P|^2 + |C_P'|^2 \qquad (3.10)
$$

$$
\alpha = |C_S|^2 + |C_S'|^2 - |C_P|^2 - |C_P'|^2 \qquad (3.11)
$$

$$
b = |C_V|^2 + |C_V'|^2 + |C_A|^2 + |C_A'|^2 \qquad (3.12)
$$

$$
\beta = |C_V|^2 + |C_V'|^2 - |C_A|^2 - |C_A'|^2 \qquad (3.13)
$$

$$
c = |C_T|^2 + |C_T'|^2 \qquad (3.14)
$$

$$
\alpha' = 2\,\mathrm{Re}(C_S C_P'^* + C_S' C_P^*) \qquad (3.15)
$$

$$
b' = 2\,\mathrm{Re}(C_V C_A'^* + C_V' C_A^*) \qquad (3.16)
$$

$$
c' = 2\,\mathrm{Re}(C_T C_T'^*) \qquad (3.17)
$$

$$
\alpha' = 2\,\mathrm{Im}(C_S C_P'^* + C_S' C_P^*) \qquad (3.18)
$$

$$
\beta' = 2\,\mathrm{Im}(C_V C_A'^* + C_V' C_A^*) \qquad (3.19)
$$

the parameters appearing in the decay probability (3.7) are given by

$$
A = a + 4b + 6c \qquad (3.20)
$$

$$
\rho = \frac{1}{A}(3b + 6c) \qquad (3.21)
$$

$$
\eta = \frac{1}{A}(\alpha - 2\beta) \qquad (3.22)
$$

$$
\xi = -\frac{1}{A}(3a' + 4b' - 14c') \qquad (3.23)
$$

$$
\delta = \frac{1}{A\xi}(-3b' + 6c') \qquad (3.24)
$$

$$
\xi' = -\frac{1}{A}(a' + 4b' + 6c') \qquad (3.25)
$$

$$
\delta' = -\frac{1}{A\xi'}(b' + 2c') \qquad (3.26)
$$

$$
\xi'' = \frac{1}{A}(3a + 4b - 14c) \qquad (3.27)
$$

$$
\rho' = \frac{1}{A\xi''}(3b - 6c) \qquad (3.28)
$$

$$
\eta' = \frac{1}{A\xi''}(3\alpha + 2\beta). \qquad (3.29)
$$

As written here, the expression (3.7) holds for μ^--decay, eq. (3.1). The corresponding decay probability for μ^+ is obtained from eq. (3.7) by charge conjugation. This amounts to change the signs of the terms in $\xi \cos\theta$ and $\xi' \cos\phi$ while leaving all other terms unaltered.

Away from threshold, i.e. for $x \gg x_0$, the terms containing x_0 and μ, the electron mass, can be

neglected. In this case our eq. (3.7) reduces to the expression given by Kinoshita and Sirlin [39]. The general analysis in terms of the real decay parameters $\rho, \eta, \ldots$ originated with L. Michel [40, 41], it was also discussed in [42].*

These rather complicated expressions simplify considerably for the case of the ideal interaction (3.6) which corresponds to the particular choice

$$C_V \equiv \frac{G}{\sqrt{2}}(\text{real}); \qquad C_A = \lambda C_V = -C'_V; \qquad C'_A = -C_V \tag{3.30a}$$

$$C_S = C'_S = C_P = C'_P = C_T = C'_T = 0.$$

Then $b = -b' = G(1 + |\lambda|^2)$, all other parameters vanishing. The parameters (3.20) to (3.29) take the simple values

$$\rho = \delta = \rho' = \tfrac{3}{4}, \qquad \xi = \xi' = \xi'' = 1$$
$$\delta' = \tfrac{1}{4}, \qquad \eta = \eta' = \alpha' = \beta' = 0 \tag{3.30b}$$

independent of the parameter λ – as expected, and

$$A = 4(1 + |\lambda|^2)G^2.$$

The parameter λ appears only in the total decay rate which is then

$$\Gamma \simeq \frac{G^2 m^5}{192\pi^3} \frac{1 + |\lambda|^2}{2} \tag{3.30c}$$

while the differential decay probability (3.7) reduces to the familiar form (we give it here for $x \gg x_0$),

$$\frac{d^2\Gamma^{(0)}(x, \theta, \phi, \psi)}{dx\, d(\cos\theta)} = \frac{m^5 G^2}{384\pi^3} \frac{1 + |\lambda|^2}{2} x^2[(3 - 2x) - (2x - 1)\cos\theta](1 - \cos\phi). \tag{3.30d}$$

Before we give the existing experimental information on these decay properties we must define the *observable quantities* pertaining to the electron as well as their relationship to the general parameters defined in eqs. (3.20) through (3.29). This will help to clarify the physical significance of the various terms in eq. (3.7).

The parameter A determines the *rate* (except for small corrections in $\eta\mu/m$ and in $(\mu/m)^2$),

$$\Gamma = \frac{Am^5}{1536\pi^3}\left\{1 + 4\eta\frac{\mu}{m} - 8\left(\frac{\mu}{m}\right)^2 + O(\mu^3/m^3)\right\}. \tag{3.31}$$

The *shape of the spectrum* of the decay electrons from unpolarized muons determines the Michel parameter ρ and the parameter η. Whilst ρ is relatively easy to obtain (up to radiative corrections, see below), the parameter η appears with the factor $\mu/m = 1/207$. Therefore, the spectrum is not very sensitive to this parameter. Also, as it is primarily the low-energy end of the spectrum which must be determined accurately, the measurement of η is a difficult experimental task. As a consequence, whilst ρ is known to about 0.4% accuracy, η, when obtained from the spectrum, is rather poorly known, as may be seen from table 3.1.

As a matter of illustration, fig. 3.2a shows the angle-independent part of the theoretical spectrum,

* See note added in proof.

Table 3.1
Muon decay parameters. The experimental values are corrected for radiative corrections

Parameter	Experiment*	"V-A"
ρ	0.752 ± 0.003	$\frac{3}{4}$
η	-0.12 ± 0.21	0
ξ	0.972 ± 0.013	1
δ	0.755 ± 0.009	$\frac{3}{4}$
P_t	-1.00 ± 0.13	-1

* Most measurements are done on μ^+-decay. We have changed the sign of P_t in these cases, in order to comply with the text where we work out μ^--decay. The complete list of references to experimental work is found in [18].

eq. (3.7), for $\eta = 0$ and for the values of ρ as indicated. The spectrum is normalized such that it is equal to ρ for $x = 1$. Fig. 3.2b shows the spectra for $\rho = \frac{3}{4}$ and three values of η. Fig. 3.2c exhibits the quantity

$$(d\Gamma(x, \eta) - d\Gamma(x, \eta = 0))/d\Gamma(x, \eta = 0)$$

near $x = x_0$. (Note that radiative corrections are not included.) Figs. 3.3a and 3.3b, finally, show two typical experimental spectra, taken from refs. [43] and [44], respectively. ξ and δ are obtained from the parity violating correlation term $\zeta_\mu \cdot \boldsymbol{p}_e$, i.e. from the *muon spin–electron momentum correlation*. Like ρ and η they are obtained from intensity measurements. The remaining observables of the electron are the three components of its polarization vector $\boldsymbol{P}$. A suitable decomposition of $\boldsymbol{P}$ is the following: Let P_t be the longitudinal component, along the electron momentum. P_{T_1} and P_{T_2} are the components perpendicular to that direction, with the choice that P_{T_1} lies in the plane determined by the muon spin and the electron momentum, whilst P_{T_2} is the component perpendicular to that plane (see fig. 3.1 insertion).

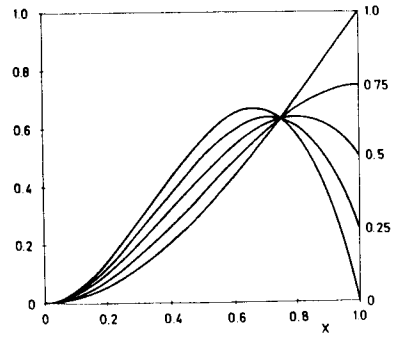

Fig. 3.2a. Michel spectra (angle independent part of expression (3.7)) for $\eta = 0$ and the values of ρ as indicated on right-hand ordinate, x: reduced electron energy, see eq. (3.4). Spectrum is normalized such that it equals ρ at $x = 1$.

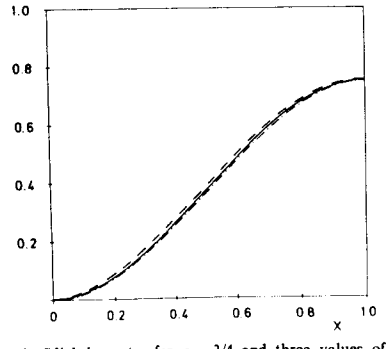

Fig. 3.2b. Michel spectra for $\rho = 3/4$ and three values of η. Solid line: $\eta = 0$; dashed line: $\eta = +1$; dot–dashed line: $\eta = -1$. Spectrum normalized as in fig. 3.2a.

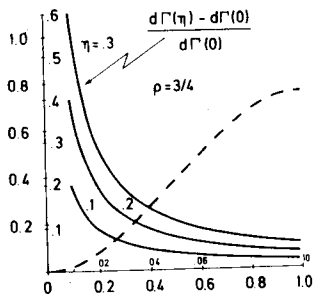

Fig. 3.2c. Dashed line: standard Michel spectrum ($\rho = 3/4$, $\eta = 0$), normalized as in figs. 3.2a and b. The lower scale on the abscissa and the left scale on the ordinate pertain to this curve. Solid lines: relative deviations of the spectrum from standard spectrum at low energies, for values of η as indicated (upper scale on abscissa, right-hand scale on ordinate). Radiative corrections are not taken into account in this figure.

The general expression of these quantities in terms of the decay parameters is obtained from eq. (3.7). We do not write down the somewhat lengthy expressions for the case of the most general four-fermion interaction.* Rather we simplify them by inserting the precise experimental information about ρ and δ that exists (cf. table 3.1). From the values $\rho = \delta = \frac{3}{4}$ we must have $a = 2c$ (eqs. (3.10) and (3.14)), and $a' = 2c'$ (eqs. (3.15) and (3.17)). It then follows that $\delta' = \frac{1}{4}$, $\rho' = \frac{3}{4}$. Neglecting the small terms in the electron mass, P_t is then given by

$$P_t = -\xi' + \frac{(2x-1)\cos\theta}{3 - 2x - \xi\cos\theta(2x-1)}\{\xi'' - \xi\xi'\} \tag{3.32}$$

(holds for $a = 2c$, $a' = 2c'$ and with $x \gg x_0$).

Furthermore, from the expressions (3.10) through (3.19) one derives the inequalities

$$-1 \leqslant \xi, \xi' \leqslant +1 \tag{3.33}$$

and

$$\xi^2 - 1 \leqslant \{\xi'' - \xi\xi'\} \leqslant 1 - \xi^2. \tag{3.34}$$

Thus, P_t depends essentially on the parameter ξ' (usually called h in the literature) whose average experimental value is shown in table 3.1. Furthermore, the absence of any energy- or θ-dependence, according to eq. (3.32) and the inequality (3.34), is a cross-check of ξ being equal to one. We note that this has not been verified experimentally so far.

P_{T_1}, the transverse component in the plane (ζ_μ, p_e), is perhaps the most interesting quantity still to be determined experimentally. With $a = 2c$, $a' = 2c'$, as above, and for $x \gg x_0$ it is given by

$$P_{T_1} \simeq \frac{4\beta + 6\alpha(1-x)}{A\{3 - 2x - \xi\cos\theta(2x-1)\}}\sin\theta. \tag{3.35}$$

* We recall that P_t, P_{T_1}, P_{T_2} are given by the ratio of the difference to the sum of $d^2\Gamma$ for ($\phi = 0$ and $\phi = \pi$), ($\phi = \pi/2$ and $\phi = -\pi/2$, with $\psi = 0$), ($\phi = \pi/2$ and $\phi = -\pi/2$, with $\psi = \pi/2$), respectively.

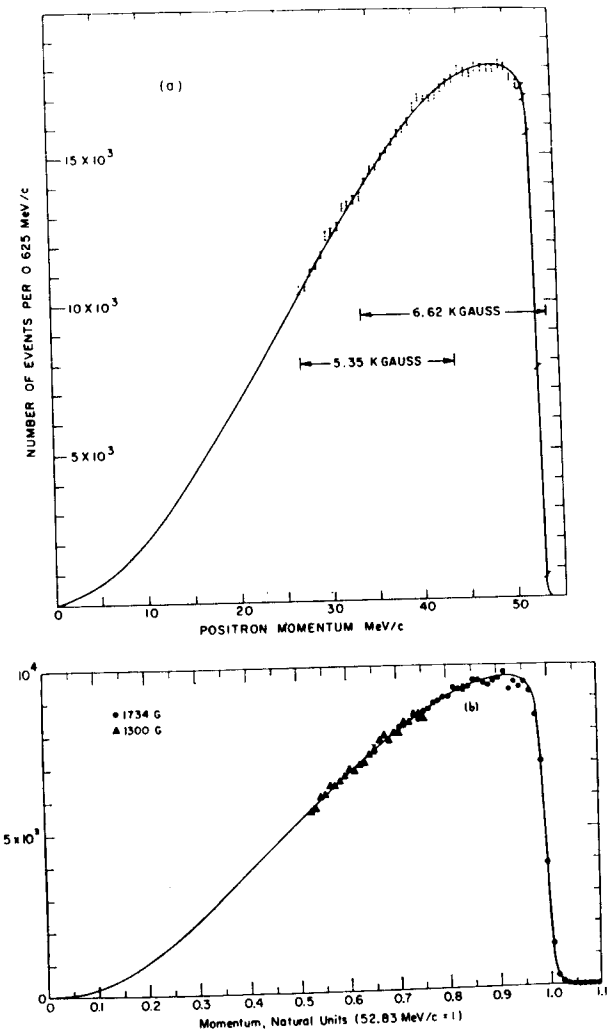

Fig. 3.3. Two experimental Michel spectra, (a) taken from [43]; (b) taken from [44].

This can be written in terms of the parameters η, η' and ξ'',

$$P_{T_1} \simeq \frac{-3\eta + \eta'\xi'' + 3(\eta + \eta'\xi'')(1-x)}{2\{3 - 2x - \xi\cos\theta(2x-1)\}}\sin\theta. \tag{3.36}$$

Thus, P_{T_1} is sensitive to deviations from pure "V-A" interaction (though the parameter β), as well as to scalar and pseudoscalar couplings (through α). If β is small (as one would expect), then η and η' are proportional to each other and P_{T_1} *essentially measures the η parameter without the disturbing suppression factors of order μ/m.*

The remaining component P_{T_2}, finally, tests time reversal invariance of the interaction (3.8). As the final state interaction is completely negligible in this case, P_{T_2} should be strictly zero if time reversal invariance holds true.

There are various special cases which could be of particular relevance and which may be studied with the aid of our formulae above. We mention two specific cases in this context.

(i) Suppose that in the charge retention form, eq. (3.8), the interaction is close to but not quite "V-A" in the electron–muon part, i.e.

$$\mathscr{H}_{\text{leptonic}} = \frac{G}{\sqrt{2}}\bar{e}\{\gamma^\alpha - (1+\varepsilon)\gamma^\alpha\gamma_5\}\mu\bar{\nu}_\mu\gamma_\alpha(1-\lambda\gamma_5)\nu_e + \text{h.c.} \tag{3.37}$$

When reordered in terms of (e, ν_e)- and (μ, ν_μ)-covariants by a Fierz transformation,

$$\sum_i (\bar{e}\Gamma_i\nu_e)(\bar{\nu}_\mu(D_i\Gamma^i + D_i'\Gamma^i\gamma_5)\mu) + \text{h.c.} \tag{3.38}$$

scalar and pseudoscalar couplings as well as the expected vector and axial–vector couplings occur in this representation*. Of course, this situation is rather unexpected on the basis of current theoretical ideas. (For instance, the branching ratio $(\pi \to e\nu)/(\pi \to \mu\nu)$ together with μ – e universality cannot tolerate large deviations from $\lambda = 1$ and $\varepsilon = 0$.) It would therefore be of great interest to give limits on such unexpected interactions from muon decay.

From our eqs. (3.10–29) we find in this case

$$\rho = \tfrac{3}{4} = \delta = \rho'; \qquad \delta' = \tfrac{1}{4}; \qquad \xi'' = 1 \tag{3.39a}$$

$$\xi = \xi' = 2\frac{1 + \operatorname{Re}\varepsilon}{1 + |1+\varepsilon|^2} \simeq 1 - \tfrac{1}{2}|\varepsilon|^2 \tag{3.39b}$$

$$\eta = -\eta' = \frac{1}{2}\frac{|1+\varepsilon|^2 - 1}{|1+\varepsilon|^2 + 1} \simeq \tfrac{1}{2}\operatorname{Re}\varepsilon. \tag{3.39c}$$

While P_t, from eq. (3.32) deviates from -1 only to order $|\varepsilon|^2$, the transverse components are *linear* in Re ε and Im ε, respectively. Indeed,

$$P_{T_1} \simeq \frac{-2\eta\sin\theta}{3 - 2x - \xi\cos\theta(2x-1)} \simeq \frac{-\operatorname{Re}\varepsilon\sin\theta}{3 - 2x - \xi\cos\theta(2x-1)} \tag{3.39d}$$

$$P_{T_2} \simeq \frac{\operatorname{Im}\varepsilon\sin\theta}{3 - 2x - \xi\cos\theta(2x-1)}. \tag{3.39e}$$

* From eq. (3.37) we find indeed $D_S = 1 - \lambda - \varepsilon\lambda$, $D_S' = -\lambda + 1 + \varepsilon$, $D_P = D_S$, $D_P' = -D_S'$, $D_V = -\frac{1}{2}(\lambda + 1 + \varepsilon\lambda) = D_A$; $D_V' = \frac{1}{2}(\lambda + 1 + \varepsilon) = D_A'$.

(ii) Suppose that in the standard charge-*changing* representation one has an interaction of the form

$$\mathscr{H}_{\text{leptonic}} = \frac{G}{\sqrt{2}}\{(\bar{e}\gamma^\alpha(1-\gamma_5)\nu_e)(\bar{\nu}_\mu\gamma_\alpha(1-\gamma_5)\mu)(1-\delta) + \delta(\bar{e}\gamma^\alpha(1+\gamma_5)\nu_e)(\bar{\nu}_\mu\gamma_\alpha(1+\gamma_5)\mu) + \text{h.c.}\} \tag{3.40}$$

with $|\delta|^2 \ll 1$.

This form of the effective interaction in μ-decay would arise if there were two (or more) different kinds of charged W-bosons coupling to left-handed and to right-handed currents, respectively [45]. In this case, we find the result (3.39a), as before. Further,

$$\xi = \xi' \simeq 1 - 2|\delta|^2. \tag{3.41a}$$

However, we now find that η and η' are exactly zero, as are the parameters α' and β' eqs. (3.18–19). Thus

$$P_{T_1} = P_{T_2} = 0. \tag{3.41b}$$

Both examples demonstrate clearly that the experimental challenge is twofold:

(i) a new precision measurement of P_t, eq. (3.32), will yield at least an upper bound for the admixture of right-handed currents or even other covariants than vector or axial vector in the purely leptonic hamiltonian.

(ii) the transverse components P_{T_1} and P_{T_2} which have not been measured so far, are more sensitive to the assumed model of the interaction. P_{T_1} essentially determines the η-parameter, without the suppression factor μ/m which hampers its determination from the spectrum. P_{T_2} tests specific violations of time reversal invariance. A non-zero result for either one of these two components would entail a major revision of our theoretical expectations about muon decay.

We now turn to the question of whether these conclusions are sensitive to radiative corrections and to corrections from W-boson propagators.

3.2. *Corrections to muon decay*

3.2.1. *Finite mass of intermediate vector bosons and/or contributions from charged Higgs scalars*

There are strong theoretical arguments in favour of the weak interactions being mediated by heavy vector bosons (charged and possibly neutral) even though these particles have not been identified experimentally to date. Indeed, the existence of intermediate vector bosons is an essential basis of renormalizable unified gauge theories of weak and electromagnetic interactions (for reviews see [46, 47, 36]). The masses of these bosons are expected to be rather high on theoretical grounds, of the order of 30–70 GeV. The existing experimental limits are of the order of 6–8 GeV. Unfortunately, this renders muon decay rather insensitive to deviations from the pure four-fermion contact interaction discussed above. If the interaction responsible for muon decay is mediated by a charged vector particle of mass m_W, then the lifetime and the decay parameters are modified by terms of the order $(m/m_W)^2$ [48]. If for instance $m_W = 10$ GeV the expected modifications are of the order of somewhat less 10^{-4}. Detecting such a small difference appears very hard with present experimental techniques. Also, at this level of precision, the radiative corrections must be calculated beyond first order in α (fine structure constant).

If there are charged scalar particles of the Higgs type with physical couplings to the leptons then these would also show up in the Michel parameter ρ. Limits are given in ref. [49].

3.2.2. Radiative corrections

So far only radiative corrections of order α have been evaluated in detail. To this order we must add the virtual photon amplitudes of figs. 3.4a–c to the decay amplitude*. Further, if experiment does not discriminate between ordinary muon decay and muon decay accompanied by the emission of a real photon, figs. 3.4d and e,

$$\mu \to e\bar{\nu}\nu\gamma \tag{3.42}$$

we must also add the amplitude for this process, integrated over the kinematically allowed domain of photon momenta, for given electron energy E_e and emission angle θ with respect to the muon spin. The interference term between these amplitudes and the non-radiative decay amplitude gives the order-α correction to the differential decay probability.

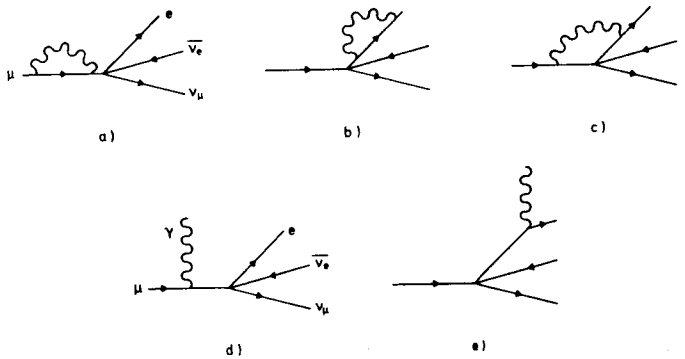

Fig. 3.4. Lowest order diagrams for radiative corrections to muon decay (a–c). Diagrams for radiative decay $\mu \to e\bar{\nu}\nu\gamma$ (d and e).

As is well-known no ultraviolet divergency occurs in these corrections as long as the weak interaction is of vector and of axial-vector type only, in the charge retention form [50, 51]. We recall that in the charge-*changing* form (3.38) such an interaction corresponds to a specific mixture of S, P, V and A interactions with

$$\begin{aligned} &D_S = D_P = C_V - C_A; \qquad D'_S = -D'_P = C'_V - C'_A \\ &D_V = D_A = -\tfrac{1}{2}(C_V + C_A); \qquad D'_V = D'_A = -\tfrac{1}{2}(C'_V + C'_A); \qquad D_T = D'_T = 0. \end{aligned} \tag{3.43}$$

For instance, the interaction (3.37) with arbitrary complex ε and λ which is a special case of this

* In general, one also has to add a soft photon emission amplitude in order to cancel the infrared divergence inherent in diagram 3.4a–c. If real photon emission is not detected the infrared divergences of fig. 3.4 cancel against those of figs. 3.4d and e automatically.

situation*, leads to convergent radiative corrections. Furthermore, as long as we average over the electron spin directions, the corrections are the same, independent of the values of the parameters ε and λ. This, however, is not so for the electron polarization: the radiative corrections to P_t, P_{T_1} and P_{T_2} do depend on ε and λ.

The radiative corrections for the case where one does not sum over electron polarization have been calculated by Fischer and Scheck [52] for the pure "V-A" case, i.e. for $\varepsilon = 0$, $\lambda = 1$ in expression (3.37). The result containing these new corrections which should be compared with eq. (3.30d) is

$$\begin{aligned} \frac{d^2\Gamma(x,\theta,\phi)}{dx\, d\cos\theta} \simeq \frac{G^2m^5}{384\pi^3}\{&[x^2(3-2x) + f_c(x)] + [x^2(1-2x) + f_\theta(x)]\cos\theta \\ &+ [-x^2(3-2x) + f_\phi(x)]\cos\phi + [-x^2(1-2x) + f_{\theta\phi}(x)]\cos\theta\cos\phi\}. \end{aligned} \tag{3.44}$$

The functions f_c, f_θ, f_ϕ and $f_{\theta\phi}$ are all proportional to α and are given by

$$f_c(x) = \frac{\alpha}{2\pi}x^2\left\{2(3-2x)R(x) - 3\ln x + \frac{1-x}{3x^2}\left[(5+17x-34x^2)\ln\left(\frac{m}{\mu}x\right) - 22x + 34x^2\right]\right\} \tag{3.45}$$

$$\begin{aligned} f_\theta(x) = \frac{\alpha}{2\pi}x^2\Bigg\{&2(1-2x)R(x) - \ln x \\ &- \frac{1-x}{3x^2}\left[(1+x+34x^2)\ln\left(\frac{m}{\mu}x\right) + 3 - 7x - 32x^2 + \frac{4(1-x)^2}{x}\ln(1-x)\right]\Bigg\} \end{aligned} \tag{3.46}$$

$$f_\phi(x) = -f_c(x) + \frac{\alpha}{6\pi}(1-x)^2(5-2x) \tag{3.47}$$

$$f_{\theta\phi}(x) = -f_\theta(x) - \frac{\alpha}{6\pi}(1-x)^2(2x+1) \tag{3.48}$$

where the function $R(x)$ stands for

$$\begin{aligned} R(x) = \left[\ln\left(\frac{m}{\mu}x\right) - 1\right]\left[2\ln\left(\frac{1-x}{x}\right) + \frac{3}{2}\right] + \ln(1-x)\left[\ln x + 1 - \frac{1}{x}\right] \\ - \ln x + 2L_2(x) - \tfrac{1}{3}\pi^2 - \tfrac{1}{2}, \end{aligned} \tag{3.49}$$

$L_2(x)$ being Euler's dilogarithm, $L_2(x) = -\int_0^x (\ln(1-t)/t)\,dt$. Note, in particular, the surprising simplicity of the results (3.47) and (3.48) which appears only at the end of a rather involved calculation [52].

In eq. (3.44) we have assumed that $x \gg x_0$ (for this reason and with the "V-A" choice of parameters the dependence on the angle ψ has disappeared from this equation). For small x the terms in x_0, x_0^2 etc. must be kept in eq. (3.44) but it is clear from our formulae how this has to be done and we do not write down this more general expression.

* See footnote on page 208.

Remember that eq. (3.44) holds for the pure "V-A" interaction. If we allow for a more complicated vector and axial-vector interaction in charge retention form, such as in eq. (3.37), then the differential decay probability (3.44) is modified according to eq. (3.7) with the parameters as given in eq. (3.39). As was noted above, the functions f_c and f_θ are not changed with these replacements. In contrast, the functions f_ϕ and $f_{\theta\phi}$, eqs. (3.47) and (3.48), are changed typically* by terms in $\alpha\varepsilon$ and $\alpha|\varepsilon|^2$ – terms, however, which turned out to be negligibly small. With this proviso we can extend eq. (3.44) to the case where the decay parameters have the values indicated in eq. (3.39).

Let us then discuss the magnitude of these corrections in view of our general analysis above. It is well known that the modification of the integrated decay width is small

$$\Gamma = \Gamma^{(0)}\left[1 + \frac{\alpha}{2\pi}\left(\frac{25}{4} - \pi^2\right)\right] \tag{3.50}$$

but that the corrections to the spectrum are rather large, of the order of 6% in the Michel parameter [50]. These are discussed in [50, 54]. The new terms in eq. (3.44) give rise to a modification of P_I due to radiative correction which is given by [52]

$$\delta P_I^{\text{rad}} \simeq \frac{\alpha}{6\pi}\frac{(1-x)^2}{x^2}\frac{5-2x-(2x+1)\cos\theta}{3-2x+(1-2x)\cos\theta}. \tag{3.51}$$

This correction is very small as long as $x \gg x_0$. Typically at $x = 0.5$ it is 0.12‰, at $x = 0.25$ it is 1.1%. It becomes large only at low electron energies, i.e. for x close to x_0, where it is of the order of 10%**.

As to P_{T_1} and P_{T_2}, the transverse components of the electron polarization, there are no corrections to these quantities except for the terms in $\alpha\varepsilon$ that we mentioned above. These terms, however, are expected to be negligible as long as the transverse components are not measured to better than, say, 1% accuracy.

3.2.3. *Further comments on radiative corrections*

We conclude our discussion on radiative corrections to muon decay with a few comments on the results presented above. Some authors have calculated radiative corrections for more general types of *four-fermion contact interactions* and also for small values of the electron energy, i.e. including the terms containing the electron mass [55, 56]. In particular, if scalar, pseudoscalar and tensor interactions are included (we refer to charge retention form) the corrections to the decay spectrum become logarithmically divergent and therefore, have to be cut off arbitrarily [56]. It is found, however, that for reasonable values of the cut-off parameter the quantitative structure of the corrections is not changed much as compared to the case of pure "V-A" interaction. The corrections to the electron polarization (P_I, P_{T_1}, P_{T_2}) have not been calculated so far for this general situation. We suspect these latter corrections to come out finite. Indeed, ultraviolet divergency stems from the *charge* radiation in the diagrams of fig. 3.4. On the other hand any modification of the electron's polarization involves a spin flip and must, therefore, stem from magnetic moment radiation. Those terms, however, are usually found to be convergent.

The radiative corrections have also been studied in the framework of theories with intermediate vector bosons. For a recent review and detailed discussion we refer to [57, 36]. As was to be

* An evaluation of these terms is in progress [53].

** If x is close to x_0, the terms in μ and in x_0 have to be kept in the decay spectrum that appears in the denominator of eq. (3.51).

expected from previous experience, it is found that the radiative corrections are essentially those of the four-fermion contact interaction, plus additional terms of the order $\alpha \cdot (m/m_W)^2$. Since such terms are negligibly small for all practical purposes, the contact interaction and the interaction mediated by heavy vector bosons are completely equivalent in calculating radiative corrections.

Finally, we should like to mention two further points which concern higher-order radiative corrections to muon decay. First, we note that the expressions still contain an infrared problem as x, the reduced electron energy, approaches its maximum $x = 1$ (where the phase space for the emission of real photons vanishes). At this point these expressions become incorrect and must be supplemented by emission amplitudes for an arbitrary number of soft photons. The resulting modifications are summarized in [57] where a complete list of references is also given. It is found that these additions would become important only for high-resolution experiments close to the upper end of the spectrum.

Second, the accuracy of the lifetime measurement eq. (2.31) is such that radiative corrections of the order $O(\alpha^2)$ may become important. Here no complete calculation has been done so far. Estimates of partial contributions [58] yield the expected order of magnitude,

$$\delta\Gamma^{(\text{2d order})} \simeq -3.5 \times 10^{-5},$$

i.e. roughly two orders of magnitude less than the corrections of order α but a complete calculation could well bring a surprise. Clearly, if one wants to extract the Fermi coupling constant G from the muon decay rate to an accuracy that is comparable to the accuracy to which the fine structure constant α is known, the second order corrections will have to be evaluated very carefully.

3.3. *Conclusions for ordinary muon decay*

Clearly the experimental situation in ordinary muon decay $\mu \to e\nu\bar{\nu}$ is not satisfactory at present (cf. table 3.1). Those parameters which are well determined, such as ρ, δ and (to a somewhat lesser extent) ξ, are compatible with a large class of interactions. For example, if one makes an unbiased least squares fit to the experimental results given in table 3.1 [59] then one finds that the data are compatible with up to roughly 30% admixture of scalar, pseudoscalar or tensor interactions (measured in coupling constants squared relative to the vector interaction) or with up to 20% deviation from one of the ratio of axial to vector couplings.

We have seen that in order to improve on this unsatisfactory state of matters precise measurements of the electron polarization components are needed. Specifically P_{T_1}, the transverse component in the plane of the muon spin and the electron momentum (which measures in essence the η parameter) is a crucial quantity for verifying the "V-A" interaction.

As we have shown, this statement is not obscured by the radiative corrections. In the kinematical domain where additional measurements can be done most easily these corrections are small and under good control. Therefore, any deviation from the simple predictions (3.30) will be a clean and direct test of the purely leptonic weak interaction.

3.4. *Radiative decay* $\mu \to e\bar{\nu}\nu\gamma$

The radiative decay

$$\mu^+ \to e^+ \nu_e \bar{\nu}_\mu \gamma \tag{3.52}$$

has a branching ratio of about 10^{-4} as compared to the ordinary decay mode (3.2). As first shown by Pratt [60] the electron and gamma ray spectra depend on the same combinations of squared coupling constants of the weak four-fermion interaction as does the ordinary decay mode. The detailed decay spectra have been worked out by Eckstein and Pratt [61] and by Fronsdal and Ueberall [62] on the basis of the general four-fermion interaction. Eckstein and Pratt also consider the effect of the vector boson mass but find again that the corrections are of order $(m/m_W)^2$. Therefore, here again the four-fermion contact interaction is adequate for discussing the information that can be obtained from this decay.

The double-differential decay probability depends on the deviations of ρ and δ from their "V-A"-value $\frac{3}{4}$ as well as on two additional real parameters $\bar{\eta}$ and κ [62].

If $\rho = \frac{3}{4} = \delta$ is accepted then these parameters are given by

$$\bar{\eta} = \frac{a/b}{2(1 + a/b)}; \qquad \kappa = -\frac{a'/b'}{2(1 - a'/b')} \tag{3.53}$$

with a, b, a' and b' as defined above in eqs. (3.10, 12, 15, 16), respectively. In this case they obey the inequalities

$$0 \leqslant \frac{\bar{\eta}}{\kappa} \leqslant \tfrac{1}{2} \tag{3.54}$$

where the lower limit applies if the interaction is the one of eq. (3.6).

Further, for ξ close to or equal to one these two parameters become equal and are in fact equivalent to P_l, the longitudinal component of the electron polarization in muon decay. This can be seen as follows: $\rho = \frac{3}{4}$ implies $a = 2c$, whilst $\delta = \frac{3}{4}$ implies $a' = 2c'$. Therefore, from eq. (3.23)

$$\xi = (a' - b')/(a + b).$$

Suppose now that $\xi = 1$ which implies $a - a' + b + b' = 0$. Since $(a - a')$ as well as $(b + b')$ are positive semi-definite by definition, we must have $a - a' = 0 = b + b'$. From this it follows that

$$1 - \xi' = \frac{a + a' + b + b'}{a + b} = \frac{2a}{a + b}$$

and therefore

$$\bar{\eta} = \kappa = \tfrac{1}{4}(1 - \xi'). \tag{3.55}$$

In this limit a measurement of these parameters is equivalent to a measurement of P_l in non-radiative muon decay, cf. eqs. (3.32, 34). It then becomes an experimental question as to which of these methods will yield the more precise result.

In the more general case ($\xi \neq 1$) the quantities $\bar{\eta}$, κ and ξ' are independent, with $\bar{\eta}$ and κ probing specifically the scalar and pseudoscalar interactions. However, as one is in fact very close to $\xi = 1$, the relation (3.55) must be true at least approximately.

An experiment by Bogart et al. gave the result [63]

$$\bar{\eta} = 0.09 \pm 0.14 \tag{3.56}$$

in agreement with the expectation. (Earlier experiments are quoted for instance in [64].) Further experiments on this decay are in progress at TRIUMF and SIN.

We note in passing that radiative corrections to radiative muon decay have been evaluated in the framework of the Weinberg–Salam model by Donnachie and Mohammad [65]. It is found that the corrections to radiative decay are exactly those which appear in normal muon decay – very much like in the older "V-A" theory.

3.5. $\mu \to e\gamma$ and muon–electron (or positron) conversion

Historically, the absence of the decay mode

$$\mu \to e + \gamma \tag{3.57}$$

as well as of the neutrinoless muon capture processes on nuclei

$$\mu^- + (Z, A) \to (Z, A)^* + e^- \tag{3.58}$$

and

$$\mu^- + (Z, A) \to (Z - 2, A)^* + e^+ \tag{3.59}$$

were important arguments for the introduction of muonic lepton number. Indeed, all three processes are forbidden with either additive or multiplicative conservation of a separate muonic lepton number L_μ (see section 2.1.3). The single lepton number scheme of Konopinski and Mahmoud with $L(e^+) = L(\mu^-)$ allows the process (3.59) but forbids processes (3.57) and (3.58). The observed suppression of $\mu^- \to e^+$ conversion then is explained by the need for a double-charge exchange in a weak process that is necessary here.

Present experimental limits are the following*

$$R_{\mu\to e\gamma} \equiv \Gamma(\mu \to e\gamma)/\Gamma(\mu \to e\nu\bar{\nu}) < 2.2 \times 10^{-8} \tag{3.60a}$$

$$R_{\mu^-\to e^-}(\mathrm{Cu}) \equiv \Gamma(\mu^-\mathrm{Cu} \to e^-\mathrm{Cu})/\Gamma(\mu^-\mathrm{Cu} \to \nu_\mu\mathrm{Ni}) < 1.6 \times 10^{-8} \tag{3.60b}$$

$$R_{\mu^-\to e^+}(\mathrm{Cu}) \equiv \Gamma(\mu^-\mathrm{Cu} \to e^+\mathrm{Co})/\Gamma(\mu^-\mathrm{Cu} \to \nu_\mu\mathrm{Ni}) < 2.6 \times 10^{-8}. \tag{3.60c}$$

The three processes are presently being studied again at the "meson factories" and at Nevis Laboratory**. The new experiments are expected to push these limits further down by one to two orders of magnitude but we cannot exclude that nonvanishing rates could be found for some of these processes. In either case their results will yield crucial clues to the understanding of leptonic weak interactions in general and muonic lepton number in particular.

In the following we discuss briefly the general analysis of $\mu \to e\gamma$ and muon–electron conversion as well as their role in the context of unified gauge theories of weak and electromagnetic interactions. We also consider negative muon–positron conversion and the implications if this process were found to occur.

3.5.1. $\mu \to e\gamma$ and $\mu^- \to e^-$ conversion

The decay $\mu \to e\gamma$ amplitude is symbolized by the vertex shown in fig. 3.5a. If this vertex function is not zero and if it is of order eG_F then the same vertex with a virtual photon line is responsible

* References for $\mu \to e\gamma$ are found in [18, 64]; $\mu^- \to e^-/e^+$ conversion was studied in [66]. References to earlier experimental work are found in [64].

** New data see note added in proof.

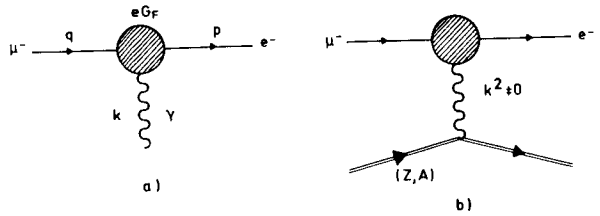

Fig. 3.5. (a) $\mu \to e\gamma$ vertex with real or virtual photon; (b) diagram for $\mu^- \to e^-$ conversion on a nucleus.

for the capture reaction (3.58). This is illustrated in fig. 3.5b.* On the basis of covariance and gauge invariance, but allowing for an arbitrary amount of parity violation, this vertex must have the form [67]

$$\langle e(p')|j^{\alpha}(0)|\mu(p)\rangle = \frac{1}{(2\pi)^3}\overline{u_e(p')}\left\{G_1(k^2)\left(\gamma^{\alpha} - k^{\alpha}\frac{m-\mu}{k^2}\right) + G_2(k^2)\left(\gamma^{\alpha} + k^{\alpha}\frac{m+\mu}{k^2}\right)\gamma_5 + \frac{i}{m}(F_1(k^2) + F_2(k^2)\gamma_5)\sigma^{\alpha\beta}k_{\beta}\right\}u_{\mu}(p). \tag{3.61}$$

Here j^{α} is the electromagnetic current operator, taken between interacting lepton states ("dressed" by weak interactions). $k_{\alpha} = p_{\alpha} - p'_{\alpha}$ is the photon momentum, m and μ denote the muon and the electron mass, respectively.

Clearly, for small k^2 the form factors G_1 and G_2 must vanish at least like k^2,

$$G_1(k^2), G_2(k^2) \sim k^2 \quad \text{for} \quad k^2 \to 0$$

in order to obtain a finite result from eq. (3.61). Therefore, only F_1 and F_2 contribute to $\mu \to e\gamma$, whilst all four form factors contribute to the capture reaction (3.58). Finally, if time-reversal invariance holds, then the hermiticity of the electromagnetic current together with T-invariance implies that all four form factors as defined through eq. (3.61) are real.**

$\mu \to e\gamma$

The differential decay probability for emission in the direction θ with respect to the muon spin direction and with the electron (positron) spin pointing in the direction ϕ with respect to its momentum (see fig. 3.6) is found to be

$$\frac{d\Gamma^{(\mp)}}{d\Omega} \simeq \frac{\alpha m}{16\pi}\{(|F_1|^2 + |F_2|^2)(1 - \cos\theta\cos\phi) \pm 2\,\mathrm{Re}(F_1F_2^*)(\cos\theta - \cos\phi)\}. \tag{3.62}$$

In eq. (3.62) the upper sign holds for μ^- decay, the lower one for μ^+ decay. Small terms of the order

* On the other hand, if the leading order is eG_F^2 then there are other competing mechanisms for reaction (3.58), involving the exchange of two intermediate vector bosons (and/or Higgs particles), without exchange of a photon. In this case, however, the rates are likely to come out very small, well below present-day experimental possibilities.

** Further general properties of these form factors under various assumptions are discussed in [68].

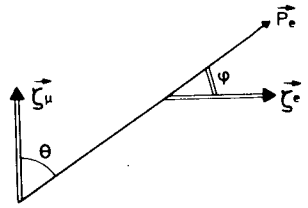

Fig. 3.6. Kinematic variables for the decay $\mu \to e\gamma$ in the muon rest system. ζ_{μ}: muon spin direction; ζ_e, p_e: electron spin and momentum direction, respectively.

of $(\mu/m)^2$ have been neglected. From eq. (3.62) the total rate is obtained by summing over the electron spin directions and by integrating over the angle θ, viz.

$$\Gamma_{\mu\to e\gamma} = \tfrac{1}{2}\alpha m(|F_1|^2 + |F_2|^2). \tag{3.63}$$

As usual parity violation manifests itself in eq. (3.62) through the spin-momentum correlation terms in $\cos\theta$ and $\cos\phi$. These terms are absent if either F_1 or F_2 vanishes identically. There is maximal parity violation if, on the contrary, $F_2 = \pm F_1$. The polarization of the outgoing electron (positron) is longitudinal (up to $(\mu/m)^2$ terms) and is given by

$$P_l^{(\mp)} = \mp 1 \pm \frac{|F_1 - F_2|^2(1 \mp \cos\theta)}{|F_1|^2 + |F_2|^2 \pm 2\,\mathrm{Re}(F_1F_2^*)\cos\theta}. \tag{3.64}$$

The upper sign holds for μ^- decay, the lower holds for μ^+ decay. If there is no parity violation, i.e. if either $F_1 \equiv 0$ or $F_2 \equiv 0$ then eq. (3.64) reduces to $P_l^{(\mp)} = -\cos\theta$. In case of maximal parity violation one has

$$P_l^{(\mp)} = \mp 1 \quad \text{for} \quad F_2 = F_1 \tag{3.65a}$$

$$P_l^{(\mp)} = \pm 1 \quad \text{for} \quad F_2 = -F_1. \tag{3.65b}$$

The first case (3.65a) corresponds to pure left-handed weak couplings, the second one, eq. (3.65b), to pure right-handed couplings.

Let us then turn to model calculations of this decay process. The situation before the setting in of renewed interest in this decay within the framework of unified gauge theories is summarized in ref. [64] and we do not go into details here. Instead we content ourselves with a few general remarks but refrain from going too much into some of the recent model considerations.

In the old days when there was only *one* neutrino, the decay $\mu \to e\gamma$ was believed to go via the diagrams shown in fig. 3.7. In general, such a model gives a logarithmically divergent decay rate [69, 70]. Only if the W-boson has an anomalous magnetic moment $\kappa_w = 1$ does the rate happen to be finite. The branching ratio is then found to be (see eq. (3.30c) with $\lambda = 1$ for the rate $\Gamma(\mu \to e\nu\bar{\nu})$)

$$R_{\mu\to e\gamma}(\nu_e \equiv \nu_{\mu}, \kappa_w = 1) = 3\alpha/4\pi = 8.7 \times 10^{-4}. \tag{3.66}$$

We note that gauge theories of the Weinberg–Salam type require precisely $\kappa_w = 1$ for the charged intermediate vector boson. However, as the electron neutrino and the muon neutrino are not identical, the diagrams of the type shown in fig. 3.7 are forbidden unless a dynamical mechanism

Fig. 3.7. Lowest order diagrams for $\mu \to e\gamma$ decay with neutrino and W-boson intermediate states only.

is introduced that breaks muon number conservation. One possibility of doing this is to assume that

(i) electron and muon couple weakly to two orthogonal linear combinations of ν_e and ν_μ, i.e. that the leptonic left-handed doublets are

$$L_e = \tfrac{1}{2}(1-\gamma_5)\begin{pmatrix} \nu_e \cos\varepsilon + \nu_\mu \sin\varepsilon \\ e \end{pmatrix}; \qquad L_\mu = \tfrac{1}{2}(1-\gamma_5)\begin{pmatrix} -\nu_e \sin\varepsilon + \nu_\mu \cos\varepsilon \\ \mu \end{pmatrix}; \tag{3.67}$$

(ii) that the two neutrinos have a nonvanishing mass difference so that at least one of them is massive. Indeed, if the neutrinos remain massless then there is no way of distinguishing the linear combinations of eq. (3.67) from the unmixed states and we may as well rename $\nu_e \cos\varepsilon + \nu_\mu \sin\varepsilon =$ "ν_e" and $-\nu_e \sin\varepsilon + \nu_\mu \cos\varepsilon =$ "ν_μ".

As long as there are no other particles in the theory the process $\mu \to e\gamma$ proceeds via the *difference* of the diagrams in fig. 3.7 taken for the ν_e intermediate state and the ν_μ intermediate state, respectively. An example for such a situation is provided by the Weinberg–Salam model in its simplest version which contains only one type of charged vector boson, one neutral vector boson and a doublet of Higgs scalars (one charged and one scalar). The neutral particles do not contribute, nor does the charged Higgs particle if a suitable gauge is chosen.

Taking the difference of these diagrams amounts to replacing the neutrino propagator $\not{p}/v^2$ in all three diagrams by* $(m^2_{\nu_\mu} - m^2_{\nu_e})\not{p}/v^4$. In this case the rate is finite even if the anomalous moment of the W-boson is not equal to one. The finiteness is not specific to gauge theories and does not require the specific relationships between coupling constants that are typical for unified gauge theories. Unfortunately the rate is found to be very small [71],

$$R_{\mu\to e\gamma}(\nu_e \not\equiv \nu_\mu) = (3\alpha/64\pi)\sin^2(2\varepsilon)\,(m^2_{\nu_\mu} - m^2_{\nu_e})^2/M_W^4. \tag{3.68}$$

Taking for instance $m_{\nu_\mu} = m_e$, $m_{\nu_e} = 0$, $M_W = 50$ GeV, and $\varepsilon = \pi/4$, this rate is smaller by twenty-one orders of magnitude than the value (3.66) obtained with identical neutrinos,

$$R(\nu_e \not\equiv \nu_\mu)/R(\nu_e \equiv \nu_\mu) \simeq 1.4 \times 10^{-21}. \tag{3.69}$$

Therefore, in such a minimal model one does not expect the decay $\mu \to e\gamma$ to occur at a measurable rate.

On the other hand, if the model is enlarged by introducing further particles such as heavy neutral [71] or charged leptons, or more species of physical Higgs particles [72], then a rate of the order of $(\alpha/\pi)^3 \simeq 1.3 \times 10^{-8}$, or of any other order of magnitude below the present experimental limit

* Up to terms of higher than second order in the neutrino masses, i.e. $O(m_1^4 - m_2^4)/v^6$.

(3.60a) can be arranged for. As long as so little is known about the masses and other properties of such new particles, these extended gauge models have little predictive power*. Only some limiting statements can be made on the basis of the known experimental upper limits for the related processes of muon-electron-conversion and the decay

$$\mu^- \to e^- e^+ e^-. \tag{3.70}$$

For the latter the latest result is [73]

$$\Gamma(\mu^- \to e^- e^+ e^-)/\Gamma(\mu^- \to e\bar{\nu}\nu) < 1.9 \times 10^{-9}. \tag{3.71}$$

If there are heavy *charged* leptons with appropriate muon-number violating couplings such as indicated in fig. 3.8 then a strong enhancement of order $(M_W/M_L)^4$ of the decay (3.70) results [74], as compared to the decay $\mu \to e\gamma$. As such an enhancement is not found experimentally this eliminates a whole class of models of this type.

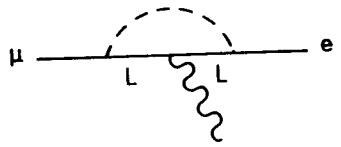

Fig. 3.8. Possible diagram for $\mu \to e\gamma$ with charged heavy lepton L in intermediate state.

$\mu^- \to e^-$ conversion

A general analysis of the exotic capture process (3.58) has been published long ago by Feinberg and Weinberg [67]. As we mentioned above this process goes predominantly via the diagram of fig. 3.5b, i.e. by exchange of a virtual photon, provided the upper vertex is allowed and is of order eG_F.** In this case the capture rate depends on all four form factors of eq. (3.61), taken at the appropriate momentum transfer (about m_μ^2 if the nucleus in the final state is not too highly excited). The rate is proportional to the quantity

$$C \equiv \{|G_1(q^2) + F_1(q^2)|^2 + |G_2(q^2) + F_2(q^2)|^2\}_{q^2 \simeq m^2}. \tag{3.72}$$

If the nuclear vertex is calculated in Born approximation and if the density of the muon bound state inside the nucleus is approximated by

$$|\phi_{1s}(0)|^2 \simeq Z_{\text{eff}}^4 m^3 \alpha^3/\pi Z$$

this rate is given by

$$\Gamma(\mu^- \to e^-) \simeq 8mZ_{\text{eff}}^4 \alpha^5 ZC\,|F(q^2 \simeq m^2)|^2 \tag{3.73}$$

where $F(q^2)$ is the elastic or inelastic electric form factor of the nucleus, depending on which final state is populated. This rate may be compared to the rate for ordinary muon capture. Within the same set of approximations this rate is given by (notation as in the book by Commins [75])

* They are in fact so flexible that they can even fit rumors.

** See first footnote on page 216.

$$\Gamma(\mu^- \to \nu_\mu) = \frac{G^2}{2\pi^2} g_V^2 (1 + 3\eta) Z_{\text{eff}}^4 m^5 \alpha^3 \tag{3.74}$$

with $g_V \simeq 1.02$

$$\eta = \frac{1}{g_V^2}(g_A^2 + \tfrac{1}{3}(g_P^2 - 2 g_A g_P)) \simeq 1.62$$

and $Z_{\text{eff}}^4 = Z^4 \int |\phi_{1s}|^2 \rho_p(r)\, d^3r / |\phi_{1s}(0)|^2$ where ϕ_{1s} is the muon wave function. The branching ratio is then given by*

$$\frac{\Gamma(\mu^- \to e^-)}{\Gamma(\mu^- \to \nu_\mu)} = \frac{16\pi^2 Z |F|^2 \alpha^2 C}{G^2 m^4 g_V^2 (1 + 3\eta)} \simeq 1.38 \times 10^{-3}\, Z |F|^2 \frac{C}{G^2 m^4} \tag{3.75}$$

with the factor C as defined in eq. (3.72).

Both for the case of ground state to ground state transition and for the sum over all excited states of the final nucleus the product: Z times form factor(s) squared, is largest for Z around 29 (copper). Also, Feinberg and Weinberg show that the coherent transition to the ground state is at least six times more frequent than the sum of transitions to all inelastic states. Therefore one expects a sharply peaked electron spectrum around the mass of the muon.

A model calculation with identical neutrinos ($\nu_e \equiv \nu_\mu$) was published by Ernst [76] who discussed in particular the question of how to suppress simultaneously $\mu \to e\gamma$ and muon–electron conversion. Other, more phenomenological analyses are quoted in [64] and we do not go into them there.

Calculations within the framework of gauge theories (and with $\nu_e \not\equiv \nu_\mu$, of course) have not been published so far. It is clear, however, that very much the same comments apply here as in the case of $\mu \to e\gamma$ (see discussion above): A model with neutrino mixing (see eq. (3.67)) will give an exceedingly small capture rate, far below the present limit (3.60b). If further particles are introduced into the model, not much can be said as long as the masses and couplings of these particles are not known from other independent information. A case to watch is probably the one sketched in fig. 3.8 with a *charged* lepton intermediate state. Here it is conceivable that an enhancement over the $\mu \to e\gamma$ process does occur, very much like in the case of the decay (3.70).**

3.5.2. $\mu^- \to e^+$ conversion on nuclei

With our present understanding of weak interactions this process seems somewhat disconnected from the processes considered in the preceding paragraph.

First, it needs a different kind of lepton number assignment and/or violation of muonic lepton number. For example the one-lepton number scheme (2.20) proposed by Konopinski and Mahmoud [30] assigns the same eigenvalue to μ^- and e^+. Therefore, in this scheme the processes (3.57), (3.58) and (3.70) are forbidden while μ^- to e^+ conversion (3.59) is allowed.

Second, the process involves a *double charge exchange* in the nucleus as two protons have to be converted into two neutrons. There are then two possibilities. Either there exist genuine isotensor weak couplings i.e. isotensor in the hadronic part of the weak coupling, in which case the process must involve mesonic or N* degrees of freedom in the nucleus. Or else, it is of higher order in weak interactions i.e. involves the exchange of two W-bosons or the like.

* See note 1 added in proof.

** See note 2 added in proof.

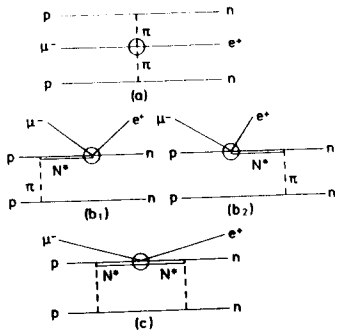

Fig. 3.9. Diagrams for $\mu^- \to e^+$ conversion on nucleons via hadronic isotensor currents.

In the first case the relevant diagrams are those of fig. 3.9 with elementary vertices of the type [77, 78]

$$\langle e^+ \pi^- | \mu^- \pi^+ \rangle \tag{3.76a}$$

$$\langle e^+ N^* | \mu^- N \rangle; \qquad \langle e^+ N | \mu^- N^* \rangle \tag{3.76b}$$

$$\langle e^+ N^* | \mu^- N^* \rangle. \tag{3.76c}$$

The first of these, eq. (3.76a) does not contribute when embedded in nuclear antisymmetric states [78]. The remaining three vertices (3.76b, c) introduce new and unknown form factors (to be taken again at $q^2 \simeq m^2$). The capture rate is then given by these effective couplings and by the probability of exciting N*-resonances in the appropriate intermediate states. Detailed expressions (though depending on further assumptions) are given in the quoted references. The experimental upper limit, eq. (3.60c), can be used to give an upper limit for isotensor couplings. It is found that such couplings (as defined in ref. [78]) must be smaller than G by at least three orders of magnitude [78]. In the second case not much can be said without a detailed analysis. In a minimal unified gauge theory analogous to the one sketched in section 3.5.1 the process could go for example via the diagram shown in fig. 3.10, where $(\nu_\mu, \bar{\nu}_e)$ and $(N_\mu, \bar{N}_e)$ denote orthogonal mixtures of ν_μ and $\bar{\nu}_e$ or some pair of heavy neutral leptons, respectively.* In this case the rate is proportional to G^4 and will therefore be by far too small to be measureable at all. Thus, as for $\mu \to e\gamma$ and $\mu^- \to e^-$ conversion we do not expect to obtain a measureable rate (i.e. a rate not much below the limit (3.60c)) from such a minimal model. We note, however, that a case where there are more weakly interacting charged particles still ought to be discussed in more detail.

A more phenomenological model with a built-in nonconservation of neutrino chirality and which yields a rate that is second order in G has been proposed and worked out by Primakoff and Rosen [79].

In conclusion, it may be fair to say that we do not expect $\mu^- \to e^+$ conversion to occur at a

* The model must of course contain left- and right-handed currents, i.e. violation of neutrino chirality.

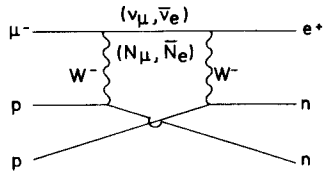

Fig. 3.10. Higher order diagram for $\mu^- \to e^+$ conversion invoking normal hadronic weak currents only.

measurable rate, on the basis of present ideas about weak interactions. Therefore, pushing down the present limit (3.60c) by further orders of magnitude would put our ideas about leptonic weak interactions on firmer ground, whereas real evidence for this process would be a major turning point in weak interaction theory, probably even more than if $\mu \to e\gamma$ were found.

4. Electromagnetic properties of the muon

This section is devoted to the electromagnetic interactions of free and bound muons. We start by summarizing the present state of the magnetic moment anomaly of the muon. We then turn to a discussion of muonium and neutral muonic helium as well as of the lightest muonic atoms such as muonic hydrogen, and muonic helium. Finally, we summarize the status of radiative corrections in medium-weight and heavy muonic atoms.

4.1. *Anomalous magnetic moment*

The anomaly of the g-factor of a spin-$\frac{1}{2}$ particle ℓ with charge -1 is defined as

$$a_\ell \equiv \tfrac{1}{2}(g_\ell - 2) \tag{4.1}$$

the relationship of g_ℓ to the magnetic moment μ_ℓ being

$$\mu_\ell = \tfrac{1}{2} g_\ell e_\ell / 2m_\ell. \tag{4.2}$$

The latest experimental value of a_μ was already quoted in section 2, eq. (2.10),

$$a_\mu = 1\,165\,922\,(9) \times 10^{-9} \tag{4.3}$$

and is obtained from the weighted average of the anomalies for positive and negative muons [20], assuming CPT-invariance. Indeed, invariance of muon interactions under CPT implies the equality of $-g_{\mu^+}$ and g_{μ^-}. Bailey et al. find the result [20]

$$(|g_{\mu^+}| - g_{\mu^-})/g = (0.026 \pm 0.017)\ \text{ppm}. \tag{4.4}$$

This is the most precise test of the CPT-theorem [80] as applied to muons.

In the light of muon physics the quantity of primary theoretical interest is the *difference* of the muon anomaly and the electron anomaly, $a_\mu - a_e$. As is well-known, to second order in e, a_μ and a_e are still equal and are given by the expression first derived by Schwinger [81]

$$a_\mu^{(2)} = a_e^{(2)} = \alpha/2\pi. \tag{4.5}$$

It is only in fourth order (order α^2) that a non-vanishing difference appears. This difference is due to the vacuum polarization graph of fig. 4.1 and is found to be [82]

$$(a_\mu - a_e)^{(4)} = \left(\frac{\alpha}{\pi}\right)^2 \left\{ \frac{1}{3} \ln\left(\frac{m_\mu}{m_e}\right) - \frac{25}{36} + \frac{\pi^2}{4}\frac{m_e}{m_\mu} - 4\left(\frac{m_e}{m_\mu}\right)^2 \ln\left(\frac{m_\mu}{m_e}\right) + \frac{134}{45}\left(\frac{m_e}{m_\mu}\right)^2 + O\left(\left(\frac{m_e}{m_\mu}\right)^3\right)\right\}. \tag{4.6}$$

From this one obtains

$$(a_\mu - a_e)^{(4)} = 1.094260675\,(\alpha/\pi)^2 = 5904.074\,(2) \times 10^{-9}. \tag{4.7}$$

A detailed discussion of all quantum electrodynamic contributions up to and including eight order as well as all other known corrections to a_μ, and many references to original work can be found in the recent review by Calmet et al. [82] from which we quote the results listed below.

The sum of all corrections due to purely electromagnetic virtual processes (involving electrons, muons and photons only) up to sixth order gives the number quoted in the first line of table 4.1.

Table 4.1
Contributions to the muon anomaly from pure QED radiative corrections as well as from higher order graphs involving also strong and weak vertices. All theoretical results taken from ref. [82]

	Contribution to a_μ times 10^9
QED 2nd, 4th and 6th order	1 165 848.1 ± 1.2
QED 8th order	3.7 ± 2.1
Strong interactions	66.7 ± 9.4
Weak interactions	2.1 ± 0.2
Total theoretical	1 165 920.6 ± 12.9
Experiment [20]	1 165 922 ± 9

This number is smaller than the experimental result, eq. (4.3) and last line of table 4.1, by the amount $(74 \pm 9) \times 10^{-9}$. The next order QED corrections, second line of table 4.1, are found to be small, of the order of $(3.7 \pm 2.1) \times 10^{-9}$. A heavy lepton L of mass 1.8 GeV/c^2 [37, 38], if it exists, contributes through a graph of the type shown in fig. 4.1, with the L replacing the electron in the closed loop, but yields only [82]

$$a_\mu\,(\text{heavy lepton with } M = 1.8\ \text{GeV}/c^2) \simeq 0.4 \times 10^{-9}. \tag{4.8}$$

In fact it turns out that the difference is due to diagrams which involve intermediate *hadronic* states. The most important contribution is due to hadronic vacuum polarization [83], fig. 4.2, and it may be expressed in terms of the total one-photon cross section $\sigma_H(t)$ for electron–positron annihilation into hadrons,

$$a_\mu^{(4)}\,(\text{hadronic}) = \frac{1}{4\pi^3} \int_{4m_\pi^2}^{\infty} \mathrm{d}t\, \sigma_H(t) \int_0^1 \mathrm{d}x\, \frac{x^2(1-x)}{x^2 + (1-x)t/m_\mu^2}. \tag{4.9}$$

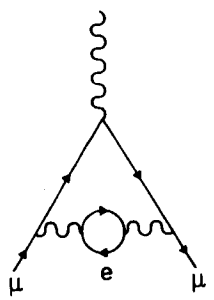

Fig. 4.1. Lowest order diagram for vacuum polarization due to virtual electron–positron loop.

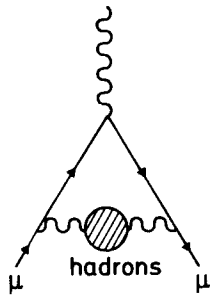

Fig. 4.2. Vacuum polarization diagram due to hadronic intermediate states.

Still higher order diagrams involving hadronic loops have also been estimated [84] but are found to be small, of the order of $(-3.5 \pm 1.4) \times 10^{-9}$. So the total hadronic contribution is about $(67 \pm 10) \times 10^{-9}$, see third line of table 4.1.

In contrast to the hadronic contributions, the contribution from graphs involving weak interaction vertices (triangular graphs with neutrino or weak boson intermediate states) is found to be small, of the order of 2×10^{-9} (fourth line of table 4.1) [82].

In conclusion, the total theoretical value is in perfect agreement with the experimental result (4.3). There is clear evidence for the hadronic contributions, as is illustrated by the numbers in table 4.1 and by fig. 4.3. This result is very impressive as it shows that the muon anomaly is predicted correctly by quantum electrodynamics and muon-electron universality up to the natural limit of quantum electrodynamics. The contribution from hadronic intermediate states is important and brings the total theoretical number into perfect agreement with experiment. There is no room left for any anomalous interaction of the muon beyond the present theoretical uncertainty of 11 ppm (which, in fact, is larger than the experimental error of 8 ppm).

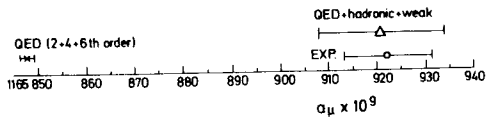

Fig. 4.3. Comparison of measured muon anomaly (open circle) with theoretical predictions. ×: theoretical value containing pure quantum electrodynamical corrections up to and including 6th order only. Δ: total theoretical value, including hadronic and weak interaction contributions.

4.2. *Muonium and light muonic atoms*

As is well-known the main motivation in studying the hyperfine structure and the Zeeman effect of muonium is to test the prediction of the muon–electron interaction by quantum electrodynamics [85, 86]. Also, as mentioned in section 2.1.1, the measurement of the hyperfine interval and the Zeeman transitions of muonium has bearing on the determination of the muon to electron charge

ratio, magnetic moment ratio and mass ratio. Clearly, this information concerns the positive muon μ^+, as it is the system μ^+e^- that is seen in experiment.

We discuss muonium (μ^+e^-) in conjunction with neutral muonic helium ($He^{++}\mu^-e^-$) because these two systems show close similarity, but are clearly distinct from muonic atoms such as μ^-p, μ^-He^{++} etc.

Both muonium and neutral muonic helium have essentially the spatial size of ordinary hydrogen

$$a_0 \simeq 1/\alpha m_e \simeq 5.3 \times 10^{-9} \text{ cm}, \tag{4.10}$$

whilst all other muonic bound systems with heavy hadronic partners have sizes about $m_e/Z \cdot m_\mu$ smaller than that. This difference in size is the reason for the qualitatively different structure of radiative corrections for these systems and it makes them, in fact, to be rather complementary in testing the predictions of QED.

That neutral muonic helium is a close relative of muonium can be realized rather easily: The muon μ^- moves very close to the He^{++} nucleus, at an orbit radius of about

$$a(\mu) \simeq 1/2\alpha m_\mu \simeq 1.3 \times 10^{-11} \text{ cm}. \tag{4.11}$$

The additional bound electron moves much further outside and, therefore, sees a screened nuclear charge of one unit only. Its orbit radius is roughly the Bohr radius (4.10) of hydrogen, very much like in muonium. Except for the motion of the μ^- in its bound state around the helium nucleus, the magnetic hyperfine interaction between the muon and the electron is rather similar in the two systems that we consider. That motion merely introduces a finite size effect into the magnetic hyperfine structure that is well-known in ordinary atomic spectra and heavy muonic atoms [87]. In our simplified discussion we first neglect this finite-size effect and treat the ($He^{++}\mu^-$) system as point-like when seen from the electron. We come back briefly to the necessary corrections at the end of subsection 4.2.2.

The behaviour of the individual hyperfine components as a function of the applied magnetic field H is given by the Breit–Rabi formula [88]

$$\nu = -\tfrac{1}{4}\Delta\nu - \frac{e_\mu}{e}|g'_\mu|\,\mu_B^\mu m_F H + (-)^{F+1}\tfrac{1}{2}\Delta\nu\sqrt{1 + 2m_F x + x^2}. \tag{4.12}$$

The dimensionless variable x is defined by

$$x = \frac{1}{\Delta\nu}\left(g_J\mu_B^e + \frac{e_\mu}{e}|g'_\mu|\,\mu_B^\mu\right)H. \tag{4.13}$$

$\Delta\nu$ is the hyperfine interval, see eq. (4.20) below. μ_B^e and μ_B^μ denote the electron and muon Bohr magneton, respectively; g_J is the electron's g-value, g'_μ the muon's g-value, both in the bound system μ^+e^-. In muonium $g_J = g_e(1 - \alpha^2/3)$ and $g'_\mu \simeq g_\mu(1 - \alpha^2/3)$.

4.2.1. *Muonium*

For muonium (M) $e_\mu/e = +1$ and $\Delta\nu_M$, see eq. (2.3) and eq. (4.20) below, is a positive quantity. In fig. 4.4a we show the curves $y(x) \equiv \nu/\Delta\nu$ as a function of x (Breit–Rabi diagram). The curves are labeled by the eigenvalues m_F of the projection of the total angular momentum F and, in the high-field Paschen–Back region, by the projections m_e and m_μ of electron spin and muon spin, respectively. Fig. 4.4b shows the same diagram but with a hypothetical muon mass of 8 MeV

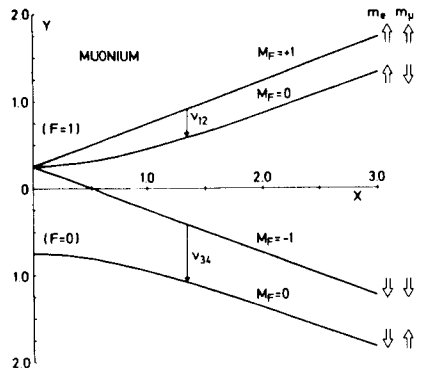

Fig. 4.4a. Breit–Rabi diagram for muonium (μ^+e^-). The abscissa x displays the standard reduced field variable, eq. (4.13).

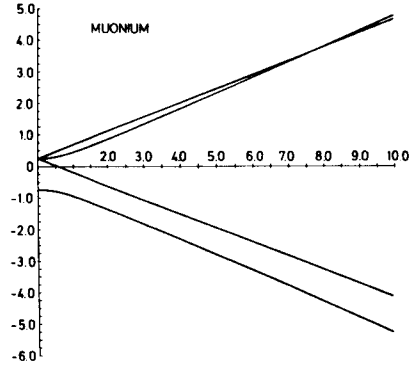

Fig. 4.4b. Same as fig. 4.4a but with hypothetical muon mass of 8 MeV in order to exhibit the level crossing of the two upper branches.

in order to exhibit the crossing of the two rising curves ($F = 1$, $m_F = 1$) and ($F = 1$, $m_F = 0$) at the point

$$x_c \simeq (r^2 - 1)/2r \qquad \text{with } r \equiv m_\mu/m_e. \tag{4.14}$$

Since the two curves also coincide at $x = 0$, this level crossing implies that the transition frequency ν_{12} between these two branches has a maximum at

$$x_\mu \simeq (r - 1)/2\sqrt{r}. \tag{4.15}$$

As is well-known, this is the essential observation of which one makes use in "field-independent" methods of measuring ν_{12} [89].

The transition frequencies ν_{12} and ν_{34} are given by, from eq. (4.12),

$$\nu_{12} = -|g'_\mu|\mu_B^\mu H + \tfrac{1}{2}\Delta\nu_M\{(1 + x) - \sqrt{1 + x^2}\} \tag{4.16}$$

$$\nu_{34} = +|g'_\mu|\mu_B^\mu H + \tfrac{1}{2}\Delta\nu_M\{(1 - x) + \sqrt{1 + x^2}\}. \tag{4.17}$$

The *sum* of these frequencies gives $\Delta\nu_M$,

$$\nu_{12} + \nu_{34} = \Delta\nu_M \tag{4.18}$$

whilst their difference can be analyzed in terms of the magnetic moment ratio μ_μ/μ_p. The result of the most recent experiment is [17]

$$\Delta\nu_M^{ex} = 4\,463\,302.35\,(.52)\,\text{kHz} \qquad (0.12\ \text{ppm}). \tag{4.19}$$

The magnetic moment ratio μ_μ/μ_p has already been quoted in section 2.1.1, eq. (2.6) above.

The current theoretical expression for $\Delta\nu_M$ is [86, 90]

$$\Delta\nu_M^{th} = \tfrac{16}{3}\alpha^2 cR_\infty \frac{\mu_\mu}{\mu_B^e}\left(1 + \frac{m_e}{m_\mu}\right)^{-3}\{1 + \tfrac{3}{2}\alpha^2 + a_e + \varepsilon_1 + \varepsilon_2 + \varepsilon_3 - \delta'_\mu\} \tag{4.20}$$

where α is the fine structure constant, R_∞ the Rydberg constant, μ_μ the magnetic moment of the muon. The various terms in the curly brackets of eq. (4.20) are the following. a_e is the electron's magnetic moment anomaly and may be taken from ref. [82] for example. The term $\frac{3}{2}\alpha^2$ is a relativistic correction to the Fermi formula, eq. (2.3). The terms ε_1, ε_2 and ε_3 are radiative corrections and are given by

$$\varepsilon_1 = \alpha^2(\ln 2 - \tfrac{5}{2}) \tag{4.21}$$

$$\varepsilon_2 = -\frac{8\alpha^3}{3\pi}\ln\alpha(\ln\alpha - \ln 4 + \tfrac{281}{480}) \tag{4.22a}$$

$$\varepsilon_3 = \frac{\alpha^3}{\pi}(18.4 \pm 5). \tag{4.22b}$$

δ'_μ, finally is a relativistic recoil correction and is given by

$$\delta'_\mu = \frac{m_e}{m_\mu}\left\{\frac{3\alpha}{\pi}\left[1 - \left(\frac{m_e}{m_\mu}\right)^2\right]^{-1}\ln\left(\frac{m_\mu}{m_e}\right) + \tfrac{5}{2}\alpha^2\ln\alpha\left[1 + \left(\frac{m_e}{m_\mu}\right)\right]^{-2}\right\}. \tag{4.23}$$

Note, in particular, the factor $\frac{5}{2}$ in front of the second term in the curly brackets of this last equation. This factor was in error until recently [91]; (in earlier publications a factor $\frac{9}{2}$ instead of $\frac{5}{2}$ was quoted).

With these formulae, using the fundamental constants as quoted in [92] and the ratio μ_μ/μ_p from eq. (2.6) one finds

$$\Delta\nu_M^{th} = \frac{\mu_\mu}{\mu_p}(1.40208237 \pm 0.8\ \text{ppm}) \times 10^6\,\text{kHz} = 4463307.3\,(6.5)\,\text{kHz} \qquad (1.5\,\text{ppm}). \tag{4.24}$$

Thus, with the experimental result (4.19) this gives for the comparison of theory and experiment

$$\Delta\nu_M^{th} - \Delta\nu_M^{ex} = 4.9\ (6.6)\,\text{kHz} \qquad (1.5\ \text{ppm}). \tag{4.25}$$

The agreement of the experimental result (4.19) with the theoretical prediction (4.24) is indeed very impressive.

4.2.2. Neutral muonic helium

For neutral muonic helium (NH) we may apply eq. (4.12) with $e_\mu/e = -1$, as a first approximation. The hyperfine interval $\Delta\nu_{NH}$ now is negative, cf. eq. (2.3), i.e. the singlet state lies higher than the triplet state. Further, as long as we neglect the difference in reduced mass corrections, the penetration of the electron into the finite spatial structure of the ($He^{++}\mu^-$) pseudonucleus and other small effects, we have

$$\Delta\nu_{NH} \simeq -\Delta\nu_M. \tag{4.26}$$

It is then natural to define $\tilde{x} = -x$, with x given by eq. (4.13) with $e_\mu/e = -1$, and to define

$$\tilde{y}(\tilde{x}) \equiv \nu/(-\Delta_{NH}).$$

Fig. 4.5a shows the Breit–Rabi diagram for neutral muonic helium, calculated from the formulae (4.12). The curves are labeled in the same way as for the Breit–Rabi diagram for muonium, fig. 4.4a. Similarly to fig. 4.4b, fig. 4.5b shows the same diagram for a hypothetical muon mass of 8 MeV

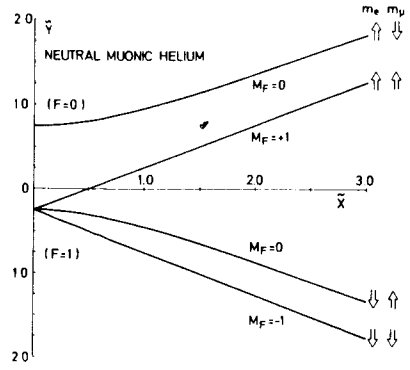

Fig. 4.5a. Breit–Rabi diagram for neutral muonic helium ($\mu^- e^- He^{++}$).

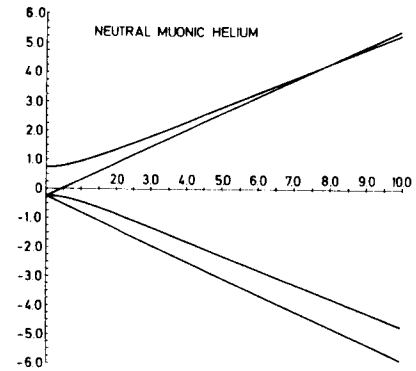

Fig. 4.5b. Same as fig. 4.5a but with $m_\mu = 8$ MeV in order to exhibit the level crossing of the two upper branches.

in order to exhibit more clearly the crossing of the two rising levels. Indeed, the levels ($F = 0$, $m_F = 0$) and ($F = 1$, $m_F = 1$) cross at about the same point where the level crossing occurs in muonium. (That this must happen is easily understood from the energies of the electron and muon dipoles in asymptotically strong magnetic fields – very much like for the case of muonium.) However, as these levels have no further intersection point, the transition frequency between them has no extremum and, consequently, there is no "magic field" as in the case of muonium.

The two following branches ($F = 1$, $m_F = 0$) and ($F = 1$, $m_F = -1$), on the other hand, do not cross, their asymptotic slopes being $-\frac{1}{2}$ and $\sim(-\frac{1}{2} - m_e/m_\mu)$, respectively.

A rather elaborate theoretical analysis of the hyperfine interval $\Delta\nu_{NH}$ has been carried through by Keh-Ning Huang [93], taking account of the effects mentioned above. He finds

$$|\Delta\nu_{NH}^{th}| = 4\,494.552\ \text{MHz}. \tag{4.27}$$

On the experimental side, neutral muonic helium has recently been identified at SREL by observation of its characteristic Larmor precession frequency [94]. The neutral system ($He^{++}\mu^- e^-$) is formed by stopping polarized muons in a high pressure gas target. The gas consists of helium and about one percent of xenon or any other gas that can act as electron donor for the formation of the neutral atom. The experiment also shows that the muon keeps some fraction of its initial polarization after having reached the 1s-state*. This fact makes it possible to perform microwave magnetic resonance experiments on this system, very much like for the case of muonium.

Such experiments are now being carried out at LAMPF and at SIN, both at low and high magnetic fields. The aim is a precision determination of $\Delta\nu_{NH}$, of the magnetic moment μ^-, and of the specific structure of the μ^-–e^- interaction in this atom. In particular, this will be the first case where the Fermi contact interaction eq. (2.3) will be tested for two particles of like charges.

If these experiments are successful one might go on to study more complicated cases such as

* It is actually found that the residual polarization is about one third of the value expected from cascade calculations. The cause for this discrepancy is not known and will be the subject of further investigations at LAMPF and SIN.

(i) one muon–multielectron atoms with spin-zero nuclei, such as μ^-Ne, μ^-Ar etc.

(ii) combined muonic and electronic hyperfine structures in atoms with non-vanishing nuclear spin, such as ($^3He^{++}\mu^- e^-$).

Theoretical investigations of such systems are still lacking.

4.2.3. Muonic hydrogen, muonic helium ($He^{++}\mu^-$) *and* ($\pi^+\mu^-$) *atom*

Muonic hydrogen (μ^-p) and muonic helium ($He^{++}\mu^-$) are the simplest muonic atoms in which radiative corrections can be studied in a rather clean and direct way. In contrast to muonium and to some extent also in contrast to neutral muonic helium ($He^{++}\mu^- e^-$) whose spatial dimension is essentially that of the ordinary hydrogen atom, the typical dimension of muonic atoms is determined by the muon's Bohr radius

$$a_B^{(\mu)} = 256\ \text{fm}/Z \tag{4.28}$$

and therefore is smaller by, roughly, a factor m_e/m_μ. As is well known this specific spatial structure causes radiative corrections in muonic atoms to be completely dominated by vacuum polarization due to virtual electron-positron pairs (cf. diagram in fig. 4.6). This is easily seen as follows. Lowest-

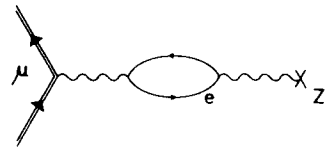

Fig. 4.6. Diagram for order $\alpha(Z\alpha)$ vacuum polarization correction for muonic bound states. Double solid line: muon bound state; single solid line: virtual electron; wavy lines: virtual photon; ×: nuclear charge (in external field approximation).

order vacuum polarization due to a virtual electron loop can effectively be written as an additional potential for the muon, viz.

$$V_{VP}(r) = -\frac{2\alpha Ze}{12\pi^2}\int d^3r'\,\frac{\rho(r')}{|r-r'|}\int_1^\infty dx\,\exp\{-2m_e x\,|r-r'|\}\left(1+\frac{1}{2x^2}\right)\frac{\sqrt{x^2-1}}{x^2} \tag{4.29}$$

where $\rho(r)$ is the charge distribution of the nucleus proton or helium in this case. This potential causes a distortion of the original static Coulomb potential of the nucleus over distances of the order of the Compton wave length of the electron

$$\lambda\!\!\!^{-}_e = 1/m_e \simeq 380\ \text{fm}. \tag{4.30}$$

Muonic orbits of low and intermediate main quantum number clearly fall within this range and, therefore, are very sensitive to this additional potential, see table 4.2 below. This is in contrast to ordinary electronic atoms whose orbits are very much larger than $\lambda\!\!\!^{-}_e$ and which therefore only feel the asymptotic tail of V_{VP}, viz.

$$V_{VP} \underset{r \gg \lambda\!\!\!^{-}_e}{\sim} \exp(-2m_e r)/r^{5/2}.$$

In electronic hydrogen, for instance, vacuum polarization contributes only about 2% to the

Table 4.2
Radiative and other contributions to muonic Lamb shift in hydrogen and helium

	${}^{1}H_{\mu}$	${}^{4}_{2}He_{\mu}$	
Contribution	Δ_3	Δ_3	Δ_1
fine structure	8.4	145.7	
VP order $\alpha Z\alpha$	204.9	1666.1	1665.8
VP higher orders	1.5	12.0	12.0
vertex correction	−0.6	−10.8	−11.1
recoil corr.		−0.2	−0.2
finite size	-3.4 ± 0.1	$-103.1\ \langle r^2\rangle$ $-102\ \langle r^2\rangle$	$-103.1\ \langle r^2\rangle$ (a) $-102\ \langle r^2\rangle$ (b)
polarizability	2×10^{-2} (c)	3.1 ± 0.6	3.1 ± 0.6
total theoretical	210.8 ± 0.1	1527.0 ± 4.2 (a)	1380.7 ± 4.2 (a)
experiment		1527.5 ± 0.3 (d)	

a) value from ref. [101]; b) value from ref. [99]; c) our own estimate. All other theoretical numbers taken from [101]. d) Experimental value from ref. [95]. All energies in meV = 10^{-3} eV.

Lamb shift which is dominated by the contribution from the vertex correction and the anomalous magnetic moment. As a consequence, the radiative corrections in muonic atoms provide new possibilities of testing the predictions of quantum electrodynamics that are complementary to hydrogen, positronium and muonium to a large extent.

In muonic hydrogen and helium the quantity of primary interest is the Lamb shift

$$\Delta_3 \equiv E(2p_{3/2}) - E(2s_{1/2}) \quad \text{or} \quad \Delta_1 \equiv E(2p_{1/2}) - E(2s_{1/2}).$$

In a pioneering experiment Zavattini and collaborators were able to measure Δ_3 in ^{4}He [95]. Their result is*

$$\Delta_3^{exp} = (1\,527.5 \pm 0.3)\ \text{meV}. \tag{4.31}$$

This number may be compared to the total theoretical prediction

$$\Delta_3^{th} = (1\,527.0 \pm 4.2)\ \text{meV} \tag{4.32}$$

to which we come back in our discussion below.

The various theoretical contributions to the muonic Lamb shift in helium and in hydrogen are calculated and discussed in [96–101]. In table 4.2 we list a sample of these results as well as the experimental result for the case of ^{4}He. Unless indicated otherwise we have taken the numbers for H from ref. [98], those for ^{4}He from the recent recalculation by E. Borie [101].

* 1 meV = 10^{-3} eV.

As is evident from the table the bulk part of the Lamb shift stems from lowest order (e^+e^-)-vacuum polarization, see fig. 4.6 and eq. (4.29). Vacuum polarization corrections of higher order than that, third line of table 4.2 (some of these are defined below in section 4.3), as well as the vertex correction, fourth line of the table, are very much smaller and, actually, have a tendency to cancel each other [101]. Among the other non-radiative corrections, the only ones that are of some importance are the shift due to the finite size of the nucleus, sixth line of table, and, for the case of ^{4}He, the shift due to the polarizability of the nucleus. The polarizability shift in helium has been debated for a while but the value (3.1 ± 0.6) meV seems now generally accepted [97, 99]. As to the finite size shift which is very important in ^{4}He, two values have been reported (see table 4.2). Using the value of ref. [101] and the r.m.s. radius of ^{4}He as obtained from electron scattering [102]

$$\langle r^2\rangle^{1/2} = (1.674 \pm 0.012)\ \text{fm}$$

one finds the results quoted in eq. (4.32) and in the table. The theoretical value Δ_3^{th} is in excellent agreement with the experimental result*:

$$\Delta_3^{th} - \Delta_3^{exp} = (-0.5 \pm 4.2)\ \text{meV}. \tag{4.33}$$

Here the error stems primarily from the uncertainty to which the helium radius is known. This sensitivity to the finite size of the helium nucleus limits somewhat the test of radiative corrections in this system. Nevertheless the agreement between theory and experiment is impressive. The vacuum polarization correction is tested to about 0.25 percent and there is clear evidence for higher-order corrections.

It should be clear from the previous discussion that the study of muonic hydrogen is of utmost importance. First, the finite size effect is much smaller than in helium. It amounts to somewhat less than two percent here, which should be compared to the 18% effect in helium. Second, the polarizability correction is very small, about 0.02 meV, and may probably be neglected altogether. At present several experiments are being carried out at CERN, LAMPF and SIN whose ultimate aim is a measurement of the Lamb shift in muonic hydrogen.

We conclude this section on light muonic atoms with a few remarks on an even simpler system: a muon bound to an oppositely charged pion:

$$(\pi^+\mu^-) \quad \text{or} \quad (\pi^-\mu^+). \tag{4.34}$$

This system which we may tentatively call "pimunium" can be formed in semileptonic decays of hadrons where there are pions and muons in the final state. "Pimunium" has recently been identified by Schwartz and collaborators [103] in the decay

$$K_L^0 \to (\pi\mu)\nu_\mu.$$

There does not seem to be any obvious way of forming the bound systems (4.34) from accelerator produced pions and muons at an appreciable rate, even with the high meson fluxes that are available at the meson factories. Therefore, an experimental study of transition energies is not an obvious experiment in the immediate future. The main theoretical interest in this system actually lies in the remark that the 2p–1s transition energy is sensitive to the radius of the pion [104].

* Using Rinker's finite size correction instead [99] one finds $\Delta_3^{th} = (1\,529.8 \pm 4.2)$ meV and $\Delta_3^{th} - \Delta_3^{exp} = (2.3 \pm 4.2)$ meV.

The reduced mass of "pimunium" is

$$\bar{m}(\mu\pi) = m_\mu m_\pi/(m_\mu + m_\pi) = 0.569 m_\mu. \tag{4.35}$$

Therefore the spatial dimension of this atom,

$$a_B(\pi^+\mu^-) = 4.50 \times 10^{-11}\ \text{cm}$$

is somewhat larger, by about a factor 2, than that of muonic atoms with nuclear partners.

4.3. *Radiative corrections in heavy and medium-weight muonic atoms*

Radiative corrections to energy levels of muonic atoms have first been studied for the case of atoms with heavy nuclei [105]. In this and in subsequent experiments [106–109] the energies of intermediate muonic transitions were measured with solid state detectors, with an accuracy that has eventually reached the level of about 23 ppm (see example quoted in table 4.3 below). It seems hard to do measurements with Ge (Li)-detectors to better than this level of accuracy. Therefore, further studies of radiative corrections in medium-weight nuclei have been started recently [110], making use of a bent-crystal spectrometer. Here accuracies of the order of a few ppm can be reached.

In all of these studies those muonic transitions are selected which are hydrogen-like to a very high degree of accuracy. On the one hand the orbits involved should lie sufficiently far outside the nucleus such that effects due to the finite size of the nucleus are small and under good control. On the other hand they should fall well inside the innermost electronic shell of the host atom so that screening of the nuclear charge by the electrons is still sufficiently small and well calculable. Good candidates are (3d–2p) and (4f–3d) transitions in light and medium weight atoms, and (5g–4f) transitions in heavy atoms.

Rather than to review the whole body of existing data we choose to discuss one typical example: the $5g_{9/2}$–$4f_{7/2}$ transition in muonic lead $^{208}_{82}Pb_\mu$. A more complete review can be found in ref. [109], see also fig. 4.7 below.

Table 4.3 shows the uncorrected transition energy, line (1), the various theoretical corrections to it, lines (2)–(9), as well as the comparison with experiment, lines (12) and (13).

Among the non-radiative corrections only the shift due to electron screening is important, see line (4). This correction has been calculated to the indicated accuracy by means of a Hartree–Fock treatment of the electronic shells [111]. The relativistic correction to the reduced-mass effect, line (2), is found to be small [112]. The finite size effect is small and can be calculated rather accurately, taking the charge parameters from electron scattering or from lower muonic transitions. The shift due to the nuclear polarizability is only known within about fifty percent (see for instance ref. [113] for discussion and further references). However, the correction is small enough so that this uncertainty does not disturb a meaningful comparison with experiment.

The lowest-order vacuum polarization, fig. 4.6 and eq. (4.29), again contributes the bulk part of the radiative corrections, line (6). This term is always *attractive* and is more effective in the 4f-orbit than in the 5g-orbit. Therefore it increases the transition energy by about two kilovolts. All higher-order corrections can be written in the form of additional potentials that may either be inserted into the Dirac equation for the muon or may be evaluated by means of perturbation theory.

Vacuum polarization of order $\alpha^2(Z\alpha)$ is given by the diagrams of fig. 4.7. These terms have been evaluated by Blomqvist and others [114] starting from the complete vacuum polarization function

Table 4.3
Radiative and other corrections for the $(5g_{9/2}\ 4f_{7/2})$ transition in muonic ^{208}Pb numbers taken from compilation [109].

	Effect	Contribution (in eV)
(1)	transition energy	429 343 (2)
(2)	reduced mass, relativistic	2
(3)	finite size	−4
(4)	screening	−83 (3)
(5)	nucl. polarizability	6 (3)
Radiative corrections:		
(6)	order $\alpha Z\alpha$	2 106 (3)
(7)	order $\alpha^2 Z\alpha$	15 (1)
(8)	orders $\alpha(Z\alpha)^{2n+1}$	−43 (2)
(9)	Lamb shift, remainder	−6 (1)
(10)	total *radiative* correction	2 072
(11)	total theoretical correction	1 993
(12)	total theoretical energy	431 336 (7)
(13)	experiment	431 334 (10)

of that order as derived earlier by Källén and Sabry [115]. Like the leading $\alpha(Z\alpha)$-term these contributions are attractive, see line (7) of table 4.3, but less than one percent of the former in magnitude.

More important is the correction due to the class of diagrams shown in fig. 4.8, with an odd number of internal photon lines connecting the electron loop and the nucleus. These diagrams are of the order $\alpha(Z\alpha)^{2n+1}$, $n = 1, 2, \ldots$, the leading term behaving as $\alpha(Z\alpha)^3$. They have first been considered by Wichmann and Kroll [116]. Exact expressions as well as power series expansions

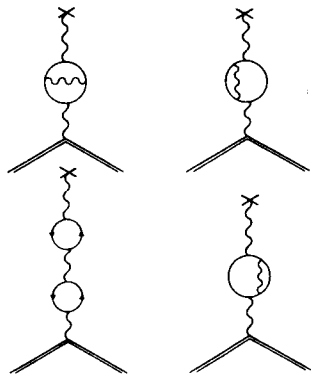

Fig. 4.7. Diagrams for vacuum polarization correction of order $\alpha^2(Z\alpha)$. Notations as in fig. 4.6.

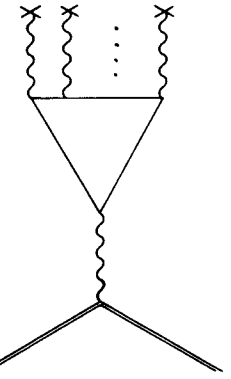

Fig. 4.8. Diagrams for order $\alpha(Z\alpha)^{2n+1}$ vacuum polarization corrections. Notations as in fig. 4.6.

of the corresponding potential term can be found in ref. [114a]. Calculations to all orders n and including the finite extension of the nuclear charge density have been published by several authors [117] who find that the finite size effect reduces this correction by about ten percent as compared to the value obtained for a point-like nuclear charge. The expansion in terms of powers of $Z\alpha$ converges rapidly, even though for lead $Z\alpha \simeq 0.6$ is not small as compared to one. Blomqvist finds [114a], for the case of lead,

$$O(\alpha(Z\alpha)^3) : O(\alpha(Z\alpha)^5) : O(\alpha(Z\alpha)^7) \simeq 1 : 0.12 : 0.02. \tag{4.36}$$

The Kroll–Wichmann correction is repulsive and its total amount is (-43 ± 2) eV in $^{208}Pb_\mu$.

The remainder of the Lamb shift (vertex correction and anomalous magnetic moment), finally, is evaluated easily [118] and is found to be small, as expected, see line (9) of the table.

In the example shown in table 4.3 the agreement of the final theoretical transition energy, line (12), with the experimental value, line (13), is excellent. Fig. 4.9 shows the difference between the calculated and the measured muonic transition energies, as a function of that energy, for all cases studied till now. The more recent experiments [107–109] are in good agreement with the theoretical predictions, but disagree with the earlier precision data of Dixit et al. [106] (open circles in the figure).

The disagreement of the early data [106] with theory had led to considerable theoretical efforts aiming at an understanding of this apparent discrepancy. On the one hand, renewed speculations about possible anomalous muon–nucleon interactions were put forward (see discussion in ref. [5]), some of which were stimulated by the need for new, possibly light particles (Higgs scalars) in unified gauge theories. For a summary of such efforts ref. [119] may be consulted.

On the other hand, there remained several QED diagrams which had not been calculated and whose order of magnitude is difficult to estimate. Specifically the contribution from virtual Del-

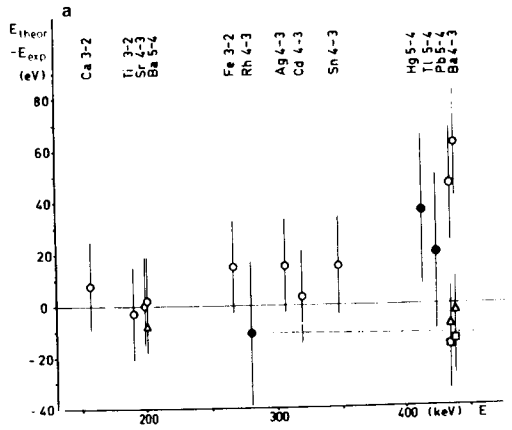

Fig. 4.9a. Difference of theoretical and experimental transition energies as function of that transition energy. Transitions n′ → n and nuclei are indicated at top of figure. Data: open circles from [106]; full circles from [109], triangles from [107], squares from [108]. Dashed line: abscissa corresponding to old value of gold calibration standard. Figure taken from [109].

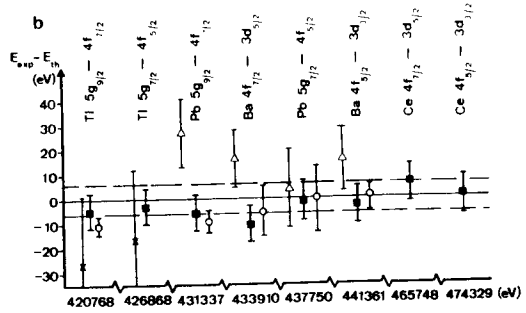

Fig. 4.9b. Difference between measured and calculated transition energies in heavy muonic atoms. Crosses from [109]; triangles from [107]; open circles from [108]. Data represented by black squares and figure taken from T. Dubler et al., preprint University of Fribourg (Sept. 77). Note that here the difference experiment minus theory is plotted, in contrast to fig. 9a.

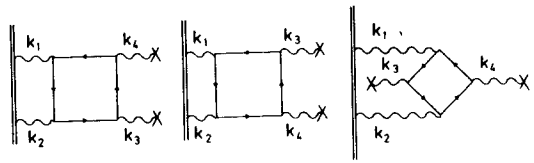

Fig. 4.10. Diagrams for order $\alpha^2(Z\alpha)^2$ vacuum polarization corrections. Notations in fig. 4.6.

brück scattering of order $\alpha^2(Z\alpha)^2$, fig. 4.10, was suspected to be important. Those diagrams have recently been evaluated very carefully [120] and have been found to give a rather small contribution, of the order of +1 eV, to the 5g–4f transition energy of muonic lead.

In conclusion, radiative corrections in heavy muonic atoms seem to be well understood and it seems unlikely that any further sizeable correction has been overlooked. The experimental situation as illustrated by fig. 4.9 is not completely satisfactory and further detailed studies seem necessary. The measurement of (3d–2p) transitions in light muonic atoms, by means of a bent-crystal spectrometer, will reduce the experimental error to a few ppm and, therefore, will be very valuable in further tests of the predictions of QED to this level of accuracy.

5. The muon as a probe

We do not know *why* the muon exists. But we have learnt, over the past twenty years, how *useful a test particle* it is in various branches of physics and in other sciences. This last section is devoted to a brief discussion of a few examples, mostly from particle physics and nuclear physics. Our discussion is necessarily somewhat fragmentary and we refer the reader to ref. [14] for a complete review up to about 1973–74. Here we prefer to review a few more recent applications (this applies to the subsection on nuclear physics) that have not been dealt with in earlier reviews.

There are several reasons which make the muon such a useful tool for the experimentalist:
(i) it is *long-lived*, the lifetime is $\tau_\mu \simeq 2.2\ \mu s$ (cf. eq. (2.31)),
(ii) all its static properties are known to great precision,
(iii) it has only weak and electromagnetic interactions with other particles, the essential features of the muon's interactions are well understood,
(iv) when produced by pion decay in flight the muon is almost fully polarized (see section 2.2.1).

5.1. Remarks on μSR (muon spin rotation)

For the purposes of *solid state physics* where one uses primarily positive muons the long lifetime permits time differential measurements of the decay asymmetry (2.37). This allows, on the one hand, to determine the Larmor precession frequency of the muon and hence the magnitude of the effective magnetic field that the muon feels in the medium. On the other hand, one can follow the time dependence of the polarization of positive muons immersed in a macroscopic medium. For example, if an external magnetic field is applied, the two spin states are split by their energy difference in that magnetic field. Any spin flip process is then accompanied by absorption or emission of an energy quantum in the solid that is to be probed. (This is called spin-lattice relaxation.) Thus rather detailed information is obtained on the interaction of the muon with static and dynamic properties of solids.

In insulators and after slowing down to thermal velocities, the positive muon catches quickly an electron to form muonium. In this case it is in fact the fate of the electrically neutral muonium atom that is being studied by the μSR (muon spin rotation) method. In metals, on the other hand, practically no muonium formation takes place. It is then the bare μ^+ which probes the medium.

The main reasons that make muons so useful for studies of solid state properties can be summarized as follows:

(i) Muons are implanted into the solid one at a time. This corresponds to the case of infinite dilution. There is no interaction between the probe particles by themselves. The disturbance of the host medium is small.

(ii) The muon causes practically no radiation damage since the stopping rate is very small. Further, if muonium is formed, this charge neutral system moves through the solid without ionizing it.

(iii) While other, more classical methods of solid state physics such as NMR and Mössbauer studies, yield information primarily about the regular lattice sites, muons are stopped almost homogeneously over the medium and thus also probe interstitial sites in the lattice.

(iv) The electric and magnetic dipole interactions of the μ^+ with the medium are simple and analysable in a transparent way.

There are further virtues of μSR methods to probe solids many of which concern primarily experimental techniques. A good introduction to these techniques can be found in [16]. For a complete review of the present state of μSR studies in solid state physics and chemistry we refer to ref. [121].

5.2. The muon in particle physics

The muon and its neutrino are of fundamental importance for particle physics, both as far as the study of their own properties and interactions is concerned as well as with regard to their use as probes of hadron physics in modern high-energy experiments.

The muon plays a key role in testing the predictions of QED and of leptonic and semileptonic weak interactions. Much of what regards weak interactions and QED has been said above, in sections 3 and 4, respectively, and shall not be repeated here. On the whole, the agreement of theoretical predictions, based on standard QED, on weak interaction phenomenology and on muon–electron universality, with recent and impressively precise measurements is excellent. Virtually all indications for possible discrepancies that had worried us for some time, have disappeared and this aspect of muon physics is well understood.

Regarding the use of muons and muon neutrinos in hadron physics there is a wealth of applications whose reviewing would go far beyond the scope of muon physics proper and, therefore, beyond the frame of this article. We content ourselves with a few remarks and refer the reader to the proceedings of recent conferences on high energy physics for information on the present state of the art.

Deep inelastic ν_μ and $\bar{\nu}_\mu$ scattering and, more recently, deep inelastic muon scattering on nucleons [122] has become a primary method of investigation of nucleonic structure functions, thus complementing the information that comes from deep inelastic electron scattering. Muons serve as indicator particles in J/ψ-spectroscopy and in searches for heavy leptons.

But also in more classical cases such as semileptonic decays of mesons and of hyperons as well as some electromagnetic decays of mesons the muonic versus electronic branching ratios are of interest. In most of those processes the energy release on the hadronic side is large as compared to the *electron* mass, but is smaller or comparable to the *muon* mass. Therefore, the *electron* behaves like a massless particle in such processes. In weak processes, in particular, it behaves like a neutrino, i.e. electrons are produced left-handed, positrons right-handed. This is not so for the *muon*, as long as its energy is not large as compared to its rest mass.

The most striking and well-known example is the decay of a (scalar or pseudoscalar) spin zero meson into a lepton pair, such as

$$\pi^\pm \to \ell^\pm \nu_\ell(\bar{\nu}_\ell), \qquad \mathrm{K}^\pm \to \ell^\pm \nu_\ell(\bar{\nu}_\ell). \tag{5.1}$$

Conservation of the z-component of total angular momentum requires the two particles in the final state to emerge with the *same* helicity. On the other hand, if the lepton ℓ has vanishing mass, then weak vector/axial vector coupling produces ℓ and ν_ℓ with *opposite* helicities, as one is a lepton while the other is an antilepton. So if $m_\ell = 0$ the decay (5.1) is forbidden. If m_ℓ is not zero, then the state vector of particle ℓ has components of both helicities and the decay (5.1) has a non-vanishing probability that is proportional to m_ℓ^2. This leads to the suppression factor (2.40) for the $e\nu_e$ branch as compared to the $\mu\nu_\mu$ branch,

$$\Gamma(\pi \text{ or } \mathrm{K} \to e\nu_e)/\Gamma(\pi \text{ or } \mathrm{K} \to \mu\nu_\mu) \simeq (m_e/m_\mu)^2. \tag{5.2}$$

This suppression factor is not specific to a "V-A" or a "V + A" coupling. It occurs for both vector and axial-vector coupling alone and, therefore, also for any mixture of V and A. The same suppression factor appears in electromagnetic decays of spin-zero mesons into a $\ell^+\ell^-$-pair. For instance, for the decay of the η meson into a lepton pair $\ell^+\ell^-$ (ℓ = e or μ), unitarity gives the following lower bound for the branching ratio with respect to the two photon decay [123, 124]

$$\frac{\Gamma(\eta \to \ell^+\ell^-)}{\Gamma(\eta \to \gamma\gamma)} \geqslant \alpha^2 \frac{m_\ell^2}{p m_\eta} \ln^2\left(\frac{m_\eta + 2p}{2m_\ell}\right) \tag{5.3}$$

where $p = \frac{1}{2}\sqrt{m_\eta^2 - 4m_\ell^2}$.

So again the e^+e^- branch is suppressed relative to the $\mu^+\mu^-$ branch by a factor of about $(m_e/m_\mu)^2$.*

5.3. Muonic atoms and nuclear physics

Muonic atoms have become an increasingly rich and precise source of information on certain aspects of nuclear structure over the last sixteen years. A detailed discussion of classical applications and of many results can be found in the reviews [113], [125]. The compilation [126] contains all data obtained with muonic atoms up to 1974. In particular, this compilation contains tables of measured charge density parameters, muonic isotope and isomer shifts, magnetic hyperfine interaction constants as well as pratical hints for evaluation of the various corrections to muonic transition energies.

In this section we turn instead to a few novel topics in muonic atoms which have been studied in some detail more recently, after completion of the reviews [125] and [113].

Muonic orbits fall into three distinct classes each of which lends itself to a specific class of applications in atomic, nuclear and particle physics:

(i) *The high-lying orbits.* These are the orbits which overlap strongly with the electronic shells of the host atom. For heavy nuclei around $Z = 82$, for example, these are the orbits with main quantum number $n \gtrsim 10$. Measurements of X-ray intensities of such high transitions (and possibly also of Auger transitions), when compared to calculations of the muonic cascade, give information on the initial population of muonic states with quantum numbers (n, l) [127]. Thus information is gained on the Coulomb capture of the muon and, thereby, on molecular or solid-state effects in the early stages of the muon's cascade.

(ii) *Intermediate orbits* which lie already well inside the electronic K-shell of the host atom but are still far enough from the nucleus so that penetration effects are still small. For such orbits the nucleus can be treated essentially as a point object with given spin J and given electromagnetic properties such as charge, (point-like) magnetic moment, electric quadrupole moment etc. These truly hydrogen-like states typically lie in the range of quantum numbers from $(n = 3, l = 2)$ to about $(n = 6, l = 5)$, depending on charge number Z.

As we have seen above, in section 4.3, these orbits are ideally suited for the study of radiative corrections, specifically vacuum polarization due to virtual electron–positron loops.

(iii) *The low-lying orbits* which penetrate strongly the nucleus. In the order of decreasing sensitivity to finite size effects these are the $1s_{1/2}$, $2s_{1/2}$, $2p_{1/2}$, and $2p_{3/2}$ states. The electromagnetic interaction energy of the muon and the nucleus in these states depends strongly on specific details of the *spatial structure* of nuclear charge and current densities.

In the past information on nuclear structure has mostly been obtained from these lowest orbits. The obvious advantage of this method is that static nuclear properties and selected nuclear transitions can be studied in presence of the negative charge cloud of the $1s_{1/2}$ muon that penetrates the nucleus deeply. This specific feature of muonic atoms gives rise to new phenomena and yields information on the nucleus that is partly complementary to information from other sources such as atomic spectroscopy, Coulomb excitation etc.

A disadvantage of the method is that the analysis of energies and intensities of transitions

* This same suppression factor m_e is the reason why $\pi^0 \to e^+e^-$ has an exceedingly small rate. In contrast to $\eta \to \mu^+\mu^-$ this process has not been seen yet [18].

between low-lying levels is model dependent to some extent. The interference of muonic and nuclear degrees of freedom is usually so intricate that some model assumption on the nuclear dynamics is needed for extracting the properties of the nucleus that one is studying. For example, one always needs some ansatz (or model prediction) for the radial dependence of charge densities, magnetization densities, electric quadrupole densities etc. Further, if there is dynamical mixing of nuclear and muonic excitations, one usually also needs a nuclear model which predicts electromagnetic transition densities between the ground state and selected nuclear excited states. As an example we quote the case of strongly deformed nuclei, where strong mixing of muonic states and rotational excitations within the nuclear ground state band can occur. In these cases one invokes the rotator model in order to relate electromagnetic transition densities to properties of the nuclear ground state. Even though the information on nuclear ground state properties extracted from muonic spectra is very precise, it still carries some model dependence whose influence is difficult to estimate quantitatively. An independent test of such model assumptions seems indicated.

For *intermediate* muonic orbits, to the contrary, muonic and nuclear dynamics are decoupled to a large extent. In the approximation of a point-like nucleus the essential quantities factorize in a muonic and a nuclear part. As the muonic matrix elements are those of an almost pure hydrogen-like atom, they can be computed to high accuracy. The nuclear quantities can thus be extracted from the data in a nearly model independent way.

An especially beautiful and novel example is the precision measurement of *spectroscopic quadrupole moments* from the hyperfine structure of intermediate muonic orbits [128–130] to which we turn in the remaining part of this section. Consider a deformed nucleus with spin $J \geqslant 1$. The charge density in the state with maximal projection quantum number $M = J$ can be expanded in terms of multipoles

$$\rho(\boldsymbol{r}) \equiv \langle JJ| \sum_{i=1}^{Z} e\delta(\boldsymbol{r} - \boldsymbol{r}_i)|JJ\rangle = \rho_0(r) + \sum_{\substack{l=2 \\ \text{(even)}}} \sqrt{\frac{4^l\pi}{2l+1}}\, \rho_l(r) Y_{l0} \tag{5.4}$$

thus defining radial multipole charge densities $\rho_l(r)$. Note that eq. (5.4) is free of any model assumption; the fact that only spherical harmonics with $m = 0$ enter here is due to the particular choice of the nuclear projection quantum number $M = J$. The factors for multipoles with $l \geqslant 2$ have been so chosen that the lth moment of the radial function $\rho_l(r)$ is equal to the corresponding multipole moment, viz.

$$\int_0^\infty \rho_2(r) r^4 \, \mathrm{d}r = eQ_s \tag{5.5}$$

$$\int_0^\infty \rho_4(r) r^6 \, \mathrm{d}r = e\pi_s. \tag{5.6}$$

Q_s and π_s are the spectroscopic quadrupole and hexadecapole moments of the nucleus, respectively. The density $\rho(\boldsymbol{r})$ is normalized to the nuclear charge, so that

$$4\pi \int_0^\infty \rho_0(r) r^2 \, \mathrm{d}r = Ze. \tag{5.7}$$

The monopole density $\rho_0(r)$ defines the spherically symmetric Coulomb potential

$$V_C(r_\mu) = -4\pi e \left\{ \frac{1}{r_\mu} \int_0^{r_\mu} \rho_0(r_N) r_N^2 \, dr_N + \int_{r_\mu}^{\infty} \rho_0(r_N) r_N \, dr_N \right\}. \tag{5.8}$$

The diagonal matrix elements of the electric quadrupole interaction in a state of total angular momentum F (vector sum of nuclear spin J and muonic angular momentum j) are given in terms of the quadrupole density $\rho_2(r)$ by the expression [131, 132]

$$W^{E2}(J; n, \kappa, \kappa; F) = \frac{3X(X-1) - 4J(J+1)j(j+1)}{2j(2j-1)J(2J-1)} A_2(J; n, \kappa, \kappa) \tag{5.9}$$

with

$$X \equiv J(J+1) + j(j+1) - F(F+1) \tag{5.10}$$

$$A_2 = A_2^{(1)} + A_2^{(2)} \tag{5.11}$$

and where

$$A_2^{(1)} = \frac{e^2 Q_s (2j-1)}{8(j+1)} \left(n'\kappa' \left| \frac{1}{r_\mu^3} \right| n\kappa \right) \tag{5.12}$$

$$A_2^{(2)} = \frac{e^2 (2j-1)}{8(j+1)} \left(n'\kappa' \left| \int_{r_\mu}^{\infty} \rho_2(r_N) \left\{ \left(\frac{r_\mu}{r_N} \right)^2 - \left(\frac{r_N}{r_\mu} \right)^3 \right\} r_N \, dr_N \right| n\kappa \right). \tag{5.13}$$

κ is the Dirac quantum number of the muonic states. The round brackets $(n'\kappa' \mid f(r_\mu) \mid n\kappa)$ denote the matrix elements taken with the *radial* muonic wave functions of the initial and final states and with the integrand $f(r_\mu)$ as indicated in eqs. (5.12) and (5.13). For the diagonal matrix elements (5.9), specifically, one has to take $n' = n$, $\kappa' = \kappa$.

Further, the quadrupole interaction in general has also large matrix elements between the two members of a given muonic fine structure doublet and must be diagonalized within this two-dimensional space. The relevant matrix elements, diagonal in the nuclear part but non-diagonal in the muonic part, can be taken from eq. (92) of the ref. [113], for example. What matters for our discussion is the fact that they are proportional to the sum $(A_2^{(1)} + A_2^{(2)})$, eqs. (5.12) and (5.13), taken with $n' = n$, but $\kappa' = -\kappa - 1$.

We have rewritten these equations in such a form as to isolate the finite size effect as far as possible. Indeed, if the nucleus is a point-like charge, i.e. if the muonic states do not penetrate into the nuclear charge, the quantity $A_2^{(2)}$ vanishes, whilst $A_2^{(1)}$ is proportional to Q_s and to the matrix element of $1/r_\mu^3$ taken between radial functions for the Coulomb potential of a point charge. The measurement of the quadrupole hyperfine structure then yields the spectroscopic quadrupole moment Q_s, without any corrections.

In reality, there is always some penetration of the muonic orbits into the nucleus. This finite size effect modifies our formulae in two ways,

(i) The radial wave functions $|n\kappa)$ pertain to the Coulomb potential $V_C(r_\mu)$, eq. (5.8), and, therefore, deviate from those pertaining to the point-charge potential $V_C^{(0)} = -Ze/r_\mu$. This is usually called *wave function distortion* effect.

(ii) There is in addition the genuine finite size term of eq. (5.13) which is due to the form of the quadrupole interaction operator.

Obviously, evaluation of these effects requires some input information on the radial densities $\rho_0(r)$ and $\rho_2(r)$. Therefore, the finite size corrections always carry some model dependence in them.

While this effect is dramatic for the *low* orbits, it is rather small, of the order of five percent, in the case of *intermediate* orbits. The way to proceed is then the following. For a chosen intermediate muonic orbit evaluate the finite size correction Δ_{FS} on A_2 by using the experimental information on $\rho(r)$ obtained from the *low* orbits (or electron scattering data, or both). Vary the charge density within the maximal limits that are compatible with those data. This provides a finite error margin δ_{FS} that reflects the model dependence of Δ_{FS}. Except for this uncertainty δ_{FS} the extraction of the spectroscopic quadrupole moment from the measured hyperfine constant A_2 is *model independent*.

In addition to the finite size effect, there are a few other small corrections which must be subtracted from the measured hyperfine structure in order to disentangle the electric quadrupole pattern proper. These corrections are discussed in detail in the thesis [128]. The most important of them is an additional energy shift due to dynamical nuclear excitation (nuclear polarizability). Other corrections such as the quadrupole part of the vacuum polarization potential, eq. (4.29), magnetic dipole and electric hexadecapole interactions, are small and can be calculated rather accurately. A typical example is the case of 4f–3d transitions in muonic lutecium for which all theoretical corrections are shown in table 5.1.

Table 5.1
Theoretical corrections to spectroscopic quadrupole moment of lutecium as obtained from muonic 4f–3d transition (numbers from ref. [128]).

Effect	Modification of Q_s (‰)*	Uncertainty (‰)
Finite size	$\Delta_{FS} = 6.3$	$\delta_{FS} = 0.5$
Nucl. polarizability	2.45	0.4
Vacuum polarization	−1.48	0.01
M1–hf interaction	0.1	$< 3 \times 10^{-3}$
E4–hf interaction	0.06	$< 10^{-2}$

* Sign convention: Q_s is shifted by indicated positive or negative amount if corresponding effect is taken into account.

Table 5.2, finally, gives the result of such an analysis of the 5g–4f, 5f–3d and 4f–3d transitions in lutecium $^{175}_{71}$Lu in the first line, as well as a comparison to the results of other methods [133–136]. In line 2 we give the value obtained from the corresponding intermediate orbits in *pionic* lutecium. This value is obtained by subtracting off the energy shift due to the nonspherical part of the strong interaction as described by the author [137]. Within the additional uncertainty to which this subtraction can be done this pionic value is also model independent. It compares very well with the independent measurement in the muonic atom.

The values obtained by means of atomic beam technique and of optical spectroscopy are quoted in lines 3 and 4 of table 5.2, respectively. The optical value is taken from the recent reevaluation by Lindgren and Rosen [135]. Neither of these values has been corrected for the Sternheimer effect which is large for this case [135]. The remaining techniques, analysis of muonic (2p–1s) transitions and Coulomb excitation, determine primarily the *intrinsic* quadrupole moment Q_0.

Table 5.2
Spectroscopic quadrupole moment of lutecium, comparison of various methods.

Method	Q_s[b]	Remarks	Reference
Intermediate muonic orbits	3.49 ± 0.02	see text	[128]
π-atom (5g–4f)	3.47 ± 0.07	strong interaction subtracted	[132]
Atomic beam	5.68 ± 0.06		[133]
Optical spectroscopy	4.67 ± 1.26		[134, 135]
Muonic (2p–1s)	3.57 ± 0.07	via rotator model	[128]
Coulomb excitation	{3.51 ± 0.07 / 3.41 ± 0.25}	via rotator model	[136]

In the case of the muonic (2p–1s) transition, moreover, some ansatz for the radial dependence of the quadrupole density $\rho_2(r)$ has been made. The spectroscopic quadrupole Q_s moment is then obtained from the intrinsic Q_0 by means of the well-known relationship of the rotator model

$$Q_s = \frac{J(2J-1)}{(J+1)(2J+3)} Q_0. \tag{5.14}$$

In contrast to the methods mentioned above, the so-obtained values for Q_s are necessarily model dependent. The fact that the results agree so well with the model independent ones is a good test of the quality of relation (5.14) and of the other model assumptions that have been made in these latter techniques.

6. Conclusions and acknowledgements

In this review of muon physics we summarize the basic static and dynamic properties of muons and their neutrinos. The concept of muon–electron universality is defined and discussed in a separate section but it is taken up again explicitly and implicitly, in many places throughout the article. Ordinary muon decay, as well as rare and ultrarare decay modes are dealt with in some detail. It is pointed out, in particular, that we are still far from having confirmed the standard theory of purely leptonic weak interactions in any definite and convincing way. In particular, the nature of muonic lepton number needs further clarification as well as the question to which extent it is conserved. We put special emphasis on key experiments that remain to be done in future studies of muon decays and which will help to confirm our ideas about the weak interactions of muons.

Regarding the electromagnetic interactions of free and bound muons we review the anomalous magnetic moment, the hyperfine interval of muonium, the Lamb shift in muonic helium and other light muonic atoms, as well as radiative corrections in heavy muonic atoms. For all of these quantities new precision data have been obtained and new calculations and/or improvements of previous calculations have been published quite recently. There is now impressive agreement between experiment and the predictions of quantum electrodynamics, without any exception. Previous discrepancies for some of these quantities have all disappeared – most of them as a result of improvements in the calculations. The only exception is the case of radiative corrections in heavy muonic atoms where recent data agree with the predictions but are in conflict with earlier precision data. This question clearly calls for further experimental study.

The last section is devoted to a brief discussion of the use of muons as probe particles in other domains of physics. Here we have selected a few examples that have not been dealt with in earlier reviews and which illustrate how powerful a tool the muon is in investigating nucleon and nuclear structure, solid state physics and chemistry.

Regarding the physics of the muon we are in a somewhat strange position. There exists a large body of precise experimental information on the muon. The description of the electromagnetic interactions of muons by quantum electrodynamics is spotless. The agreement between theory and experiment is perfect up to the natural limit of quantum electrodynamics. Although the data on the muon's *weak* interactions are incomplete and much less precise, so far all observations are consistent with the "V-A" interaction. So we dispose of a very good theory to describe the interactions of the muon. Nevertheless we know very little about the muon's *role* within the general frame of physics. Very few phenomena in nature would be affected, to the best of our knowledge, if the muon did not exist. Charged pions would have a lifetime of about 10^{-3} sec instead of 2.6×10^{-8} sec but that would not modify the properties of nuclei and therefore of stable matter in any decisive way.

From that point of view the muon is superfluous. The existence of a heavy electron looks like a whim of nature rather than a real necessity for the structure of matter. To some extent this reminds us of the state of knowledge about electricity and magnetism in the late eighteenth century. The electric and magnetic phenomena known at that time were considered to be somewhat mysterious curiosities but did not seem to be of much practical use. Magnetic matter (the famous Mesmer stones) were believed to cure from illness [138]; B. Franklin's lightning-rods were used to protect houses from the damage of thunderstorms. But otherwise electricity was felt to be a somewhat superfluous though curious phenomenon. For the sake of illustration we refer to a famous book by Charles Burney, the musicologist [139]. In the foreword to his book on the present state of music in France and Italy he compares music to the phenomena of electricity and explains that music is so much more useful to men than electricity ...*

As we all know, a little more than half a century later electrodynamics was discovered and was found to play a central role in the development of physics.

In this sense we wish to conclude by expressing our strong hope that the muon and its neutrino will appear less "curious", and that their role in physics will be understood much better in a near future. It is likely that a clarification of the nature of the lepton numbers as well as the unification of weak and electromagnetic and strong interactions will be among the keys to a better understanding of the place of the muon in nature.

I wish to thank Gerry Brown and Jim Hamilton for their warm encouragement to write up this report. I have benefitted a lot from many discussions with my colleagues of the theory group at SIN and at Mainz University. Special thanks go to J. Missimer who suggested many improve-

* "Electricity is universally allowed to be a very entertaining and surprising phenomenon, but it has frequently been lamented that it has never yet, with much certainty, been applied to any very useful purpose. The same reflexion has often been made, no doubt, as to music. [.....] ... in England, perhaps more than in any other country, it is easy to point out the humane and important purposes to which [music] has been applied. [...] Many an orphan is cherished by its influence. The pangs of child-birth are softened and rendered less dangerous and dreadful by the effect of its power. It helps, perhaps, to stop the ravages of a disease which attacks the very source of life. [.....] ... at present it is so combined with things sacred and important, as well as with our pleasures, that mankind seems wholly unable to subsist without it."

ments on the manuscript. Last but not least I would like to thank my experimental colleagues of the MEPOL group* for introducing me to the secrets of experimental particle physics during many night shifts at SIN. Finally, we thank Mrs. H. Glöß for her care in typing and preparing the various versions of this manuscript.

Appendix on notation and conventions

Except for some formulae in section 2.1 where the factors h and c are written out explicitly, natural units

$$\hbar = c = 1 \tag{A.1}$$

are assumed throughout.

We use the standard metric

$$g^{00} = +1; \qquad g^{ii} = -1 \qquad (i = 1, 2, 3). \tag{A.2}$$

One particle states of momentum $\boldsymbol{p}$ are normalized thus

$$\langle \boldsymbol{p}' | \boldsymbol{p} \rangle = 2p_0 \delta(\boldsymbol{p}' - \boldsymbol{p}) \tag{A.3}$$

for bosons and for fermions. For fermions there is an additional Kronecker symbol for the spin indices, so that in terms of Dirac spinors, one has

$$\overline{u^{(r)}(\boldsymbol{p})} u^{(s)}(\boldsymbol{p}) = 2m\delta_{rs}.$$

The definition of the Dirac matrices is the standard one (consult for example the book on relativistic quantum mechanics by Bjorken and Drell). Specifically

$$\gamma_5 = i\gamma^0\gamma^1\gamma^2\gamma^2.$$

Except in section 3 the masses of the muon and the electron are written explicitly as m_μ and m_e, respectively. In section 3 we have preferred to denote the muon mass by m, the electron mass by μ, for convenience.

Notes added in proof

Note to p. 204

The fact that the decay spectrum was continuous, i.e. that muon decay is a three body decay, was proved in an early experiment by J. Steinberger (Phys. Rev. 74 (1948) 500; 75 (1949) 1136).

Note to p. 215

In the meantime two experimental groups at SIN have published new and improved upper limits on the processes (3.57)–(3.59). Their results are

(i) $R_{\mu^- \to e\gamma} < 1.1 \times 10^{-9}$. (A1)

* Measurement of the electron polarization in muon decay.

This experiment was carried out by a group from ETH Zurich and SIN (H.P. Povel et al., Phys. Letters 72B (1977) 183).

(ii) $R_{\mu^- \to e^-}(\mathrm{S}) < 4 \times 10^{-10}$ (90% C.L.). (A2)

This result on sulfur was obtained by a group from Berne University (A. Badertscher et al., Phys. Rev. Letters 39 (1977) 1385).

(iii) The Berne group has also searched for $\mu^- \to e^+$ conversion on sulfur. Their result is

$$R_{\mu^- \to e^+}(\mathrm{S}) < 1 \times 10^{-9} \qquad (90\%\ \mathrm{C.L.}) \tag{A3}$$

(private communication from B. Hahn, and to be published in Phys. Letters).

Notes to p. 220

1. The normal muon capture rate is further suppressed by Pauli blocking and by the squared ratio of mean neutrino energy to muon mass. See erratum to [67] in Phys. Rev. Letters 3 (1959) 244 and [75] for details.

2. In a more recent publication Marciano and Sanda have studied this case in some detail (Phys. Rev. Letters 38 (1977) 1512). They find, indeed, that in many models $\mu^- \to e^-$ conversion is enhanced as compared to the decay $\mu \to e\gamma$, even more than the decay mode $\mu \to e\bar{e}e$. This corroborates the expectation that neutrinoless muon capture is a most sensitive test reaction to violation of muonic lepton number.

References

[1] (a) C.D. Anderson and S.H. Neddermeyer, Phys. Rev. 50 (1936) 263.
(b) C.D. Anderson and S.H. Neddermeyer, Phys. Rev. 51 (1937) 884.
(c) C.D. Anderson and S.H. Neddermeyer, Phys. Rev. 54 (1938) 88. (Further references to early experimental work are found in this work.)
[2] H. Yukawa, Proc. Phys. Math. Soc. Japan 17 (1935) 48.
[3] M. Conversi, E. Pancini and O. Piccioni, Phys. Rev. 71 (1947) 209.
[4] S. Tomonaga and G. Araki, Phys. Rev. 58 (1940) 90.
[5] L.B. Okun and V.J. Zakharov, Nucl. Phys. B57 (1973) 252.
[6] W.Y. Chang, Rev. Mod. Phys. 21 (1949) 166; see also references quoted in [7].
[7] V.L. Fitch and J. Rainwater, Phys. Rev. 92 (1953) 789.
[8] R.L. Garwin, L.M. Lederman and M. Weinrich, Phys. Rev. 105 (1957) 1415.
[9] J.I. Friedman and V.L. Telegdi, Phys. Rev. 105 (1957) 1681.
[10] (a) J.A. Wheeler, Rev. Mod. Phys. 21 (1949) 133.
(b) J.A. Wheeler, Phys. Rev. 92 (1953) 812.
[11] E. Fermi and E. Teller, Phys. Rev. 72 (1947) 399.
[12] (a) L. Wilets, Dan. Mat. Fys. Medd. 29, No. 3 (1954).
(b) B.A. Jacobson, Phys. Rev. 96 (1954) 1637.
[13] J. Tiomno and J.A. Wheeler, Rev. Mod. Phys. 21 (1949) 153.
[14] V. Hughes and C.S. Wu, eds., Muon Physics Vol. I–III (Academic Press, New York 1975).
[15] N. Mukhopadhyay, Physics Reports 30C (1977) No. 1.
[16] A. Schenck, in: Nuclear and Particle Physics at Intermediate Energies, ed. J.B. Warren (Plenum Press, New York 1976).
[17] D.E. Casperon et al., Phys. Rev. Letters 38 (1977) 956, 38 (1977) 1504.
[18] Review of Particle Properties, Rev. Mod. Phys. 48 (1976) No. 2.
[19] K.M. Crowe et al., Phys. Rev. D5 (1972) 2145.
[20] J. Bailey et al., Phys. Letters 67B (1977) 225.
[21] A.R. Clark et al., Phys. Rev. D9 (1974) 533.
[22] H. Anderhub et al., SIN Jahresbericht 1976.

[23] (a) L.G. Hyman et al., Phys. Letters 25B (1967) 376.
(b) E.V. Shrum and K.O.H. Ziock, Phys. Letters 37B (1971) 115.
(c) P.S.L. Booth et al., Phys. Letters 26B (1967) 39; 32B (1970) 723.
(d) M. Daum et al., Phys. Letters 60B (1976) 380.
(e) M. Daum et al., SIN Physics Report No. 1 (1976).
[24] M. Ruderman et al., Phys. Rev. 132 (1963) 1227.
[25] N. Straumann, Neutrino Emission and Stellar Evolution, in: Proc. of Spring School on Weak Interactions and Nuclear Structure (SIN April 1972).
[26] G. Backenstoss, B.D. Hyams, G. Knop, P.C. Marin and U. Stierlin, Phys. Rev. Letters 6 (1961) 415;
M. Bardon, P. Franzini and J. Lee, Phys. Rev. Letters 7 (1961) 23.
[27] G. Danby, J.M. Gaillard, K. Goulianos, L.M. Lederman, N. Mistry, M. Schwartz and J. Steinberger, Phys. Rev. Letters 9 (1962) 36;
J. Bienlein et al., Phys. Letters 13 (1964) 80.
[28] G. Feinberg and S. Weinberg, Phys. Rev. Letters 6 (1961) 381.
[29] T. Eichten et al., Phys. Letters 46B (1973) 281.
[30] E.J. Konopinski and H.M. Mahmoud, Phys. Rev. 92 (1953) 1045.
[31] B.H. Wiik and G. Wolf, Electron-Positron Interactions, Lectures at Les Houches Summer School 1976; DESY preprint 77/01.
[32] M.P. Balandin et al., JETP 40 (1974) 811.
[33] B. Hahn, J. Schacher and G.M. Viertel, SIN Jahresbericht 1976.
[34] T. Kinoshita, Phys. Rev. Letters 2 (1959) 477.
[35] (a) E. Di Capua et al., Phys. Rev. 133 (1964) B1333.
(b) D. Bryman and C. Picciotto, Phys. Rev. 11D (1975) 1337.
[36] M.A.B. Bég and A. Sirlin, Ann. Rev. Nucl. Sci. 24 (1974) 579.
[37] M.L. Perl et al., Phys. Rev. Letters 35 (1975) 1489;
M.L. Perl et al., Phys. Letters 63B (1976) 466; 70B (1977) 487.
[38] J. Burmester et al., DESY preprints 77/24 and 77/25;
G. Flügge, DESY preprint 77/35.
[39] T. Kinoshita and A. Sirlin, Phys. Rev. 108 (1957) 844.
[40] L. Michel, Proc. Phys. Soc. A63 (1950) 514.
[41] C. Bouchiat and L. Michel, Phys. Rev. 106 (1957) 170.
[42] C. Jarlskog, Nucl. Phys. 75 (1966) 659.
[43] M. Bardon et al., Phys. Rev. Letters 14 (1965) 449.
[44] B.A. Sherwood, Phys. Rev. 156 (1967) 1475.
[45] J.C. Pati and A. Salam, Phys. Rev. Letters 31 (1973) 661.
[46] J. Bernstein, Rev. Mod. Phys. 46 (1974) 7.
[47] E. Abers and B.W. Lee, Phys. Reports 9C (1973) 1.
[48] T.D. Lee and C.N. Yang, Phys. Rev. 108 (1957) 1611.
[49] P. Fayet, Nucl. Phys. B78 (1974) 14.
[50] (a) S.M. Berman, Phys. Rev. 112 (1958) 267.
(b) T. Kinoshita and A. Sirlin, Phys. Rev. 113 (1959) 1652.
(c) G. Källén, Springer Tracts in Mod. Phys. 46 (1968) 67.
[51] S.M. Berman and A. Sirlin, Ann. Phys. (N.Y.) 20 (1962) 20.
[52] W.E. Fischer and F. Scheck, Nucl. Phys. B83 (1974) 25.
[53] M.T. Mehr and F. Scheck, to be published.
[54] B.A. Sherwood, Phys. Rev. 156 (1967) 1475.
[55] H. Grotch, Phys. Rev. 168 (1968) 1872.
[56] V. Florescu and O. Kamei, Nuovo Cim. A56 (1968) 967.
[57] A.M. Sachs and A. Sirlin, in: Muon Physics, eds. C.S. Wu and V. Hughes (Academic Press, New York 1975) Chap. V, 2.
[58] M. Roos and A. Sirlin, Nucl. Phys. B29 (1971) 296.
[59] S. Derenzo, Phys. Rev. 181 (1969) 1854.
[60] R.H. Pratt, Phys. Rev. 111 (1958) 649.
[61] S.G. Eckstein and R.H. Pratt, Ann. Phys. (N.Y.) 8 (1959) 297.
[62] C. Fronsdal and H. Uberall, Phys. Rev. 113 (1959) 654.
[63] E. Bogart et al., Phys. Rev. 156 (1967) 1405.
[64] S. Frankel, Rare and Ultrarare Muon Decays, in: Muon Physics Vol. II, eds. V. Hughes and C.S. Wu (Academic Press, New York 1975).
[65] A. Donnachie and J. Mohammad, preprint CERN TH. 2132 (1976).
[66] D.A. Bryman et al., Phys. Rev. Letters 28 (1972) 1469.

[67] G. Feinberg and S. Weinberg, Phys. Rev. Letters 3 (1959) 111.
[68] Wu Ki Tung, Phys. Letters 67B (1977) 52.
[69] M.E. Ebel and F.J. Ernst, Nuovo Cim. 15 (1960) 173.
[70] Ph. Meyer and G. Salzmann, Nuovo Cim. 14 (1959) 1310.
[71] T.P. Cheng and Ling Fong Li, Phys. Rev. Letters 38 (1977) 381.
[72] J.D. Bjorken and S. Weinberg, Phys. Rev. Letters 38 (1977) 622.
[73] S.M. Korenchenko et al., JETP 43 (1976) 1.
[74] W.J. Marciano and A.J. Sanda, Phys. Letters 67B (1977) 303.
[75] E.D. Commins, Weak Interactions (McGraw-Hill, New York 1973).
[76] F.J. Ernst, Phys. Rev. Letters 5 (1960) 478.
[77] L.S. Kisslinger, Phys. Rev. Letters 26 (1971) 998; 28 (1972) 869.
[78] M. Rho and M.D. Shuster, Phys. Letters 42B (1972) 45.
[79] H. Primakoff and S.P. Rosen, Phys. Rev. D5 (1972) 1784.
[80] G. Lüders, Ann. Phys. (N.Y.) 2 (1957) 1;
R. Jost, Helv. Phys. Acta 30 (1957) 409 and 36 (1963) 77.
[81] J. Schwinger, Phys. Rev. 73 (1948) 416 L.
[82] J. Calmet et al., Rev. Mod. Phys. 49 (1977) 21.
[83] B.E. Lautrup, A. Peterman and E. de Rafael, Phys. Reports 3C (1972) 193.
[84] J. Calmet et al., Phys. Letters 61B (1976) 283.
[85] V.W. Hughes, Ann. Rev. Nucl. Sci. 16 (1966) 445.
[86] S.J. Brodsky and S.D. Drell, Ann. Rev. Nucl. Sci. 20 (1970) 147.
[87] A. Bohr and V.F. Weisskopf, Phys. Rev. 77 (1950) 94.
[88] G. Breit and J. Rabi, Phys. Rev. 38 (1931) 2082;
N.F. Ramsey, Molecular Beams (Clarendon Press, Oxford 1969).
[89] R.D. Ehrlich et al., Phys. Rev. A5 (1972) 2357.
[90] S.J. Brodsky and G.W. Erickson, Phys. Rev. 148 (1966) 26.
[91] G.P. Lepage, preprint SLAC-PUB-1900 (quoted in erratum to ref. [17]).
[92] E.R. Cohen and B.N. Taylor, J. Phys. Chem. Ref. Data 2 (1973) 663;
T.W. Hänsch et al., Phys. Rev. Letters 32 (1974) 1336.
[93] Keh-Ning Huang, Dissertation Yale University 1974.
[94] P.A. Souder et al., Phys. Rev. Letters 34 (1975) 1417.
[95] A. Bertin et al., Phys. Letters 55B (1975) 411;
G. Carboni et al., Nuovo Cim. 34A (1976) 493;
G. Carboni et al., Nucl. Phys. A278 (1977) 381.
[96] E. Campani, Nuovo Cim. Lettere 4 (1970) 982.
[97] J. Bernabeu and C. Jarlskog, Nucl. Phys. B75 (1974) 59; Phys. Letters 60B (1976) 197.
[98] E. Borie, Z. Physik A275 (1975) 347.
[99] G.A. Rinker, Phys. Rev. A14 (1976) 18.
[100] E.M. Henley et al., Nucl. Phys. A256 (1976) 349.
[101] E. Borie, preprint TKP 77-13, University of Karlsruhe, July 77.
[102] I. Sick et al., Phys. Letters 64B (1976) 33.
[103] R. Coombes et al., Phys. Rev. Letters 37 (1976) 249.
[104] L.L. Nemenov, JETP 15 (1972) 582;
U. Bar-Gadda and C.F. Cho, Phys. Letters 46B (1973) 95.
[105] G. Backenstoss et al., Phys. Letters 31B (1970) 233.
[106] M.S. Dixit et al., Phys. Rev. Letters 27 (1971) 878.
[107] L. Tauscher et al., Phys. Rev. Letters 35 (1975) 410.
[108] M.S. Dixit et al., Phys. Rev. Letters 35 (1975) 1633; 39 (1977) 307.
[109] J.L. Vuilleumier et al., Z. Physik A278 (1976) 109.
[110] R. Eichler, thesis ETH Zürich 1976.
[111] P. Vogel, Phys. Rev. A7 (1973) 63.
[112] J.L. Friar and J.W. Negele, Phys. Letters 46B (1973) 5;
R.C. Barrett et al., Phys. Letters 47B (1973) 297.
[113] J. Hüfner, F. Scheck and C.S. Wu, Muonic Atoms, in: Muonic Physics Vol I, eds. V. Hughes and C.S. Wu (Academic Press, New York 1975).
[114] (a) J. Blomqvist, Nucl. Phys. B48 (1972) 95; see also
(b) M.K. Sundersan and P.J.S. Watson, Phys. Rev. Letters 29 (1972) 15; 29 (1972) 1122.
(c) T.L. Bell, Phys. Rev. A7 (1973) 1480.

[115] G. Källén and A. Sabry, Dan. Mat. Fys. Medd. 29 (1955) No. 17.
[116] E.H. Wichmann and N.M. Kroll, Phys. Rev. 101 (1956) 843.
[117] J. Arafune, Phys. Rev. Letters 32 (1974) 560;
L.S. Brown et al., Phys. Rev. Letters 32 (1974) 562;
M. Gyulassy, Phys. Rev. Letters 32 (1974) 1393;
G.A. Rinker and L. Wilets, Phys. Rev. A12 (1975) 748.
[118] R.C. Barrett et al., Phys. Rev. 166 (1968) 1589.
[119] L. Resnick et al., Phys. Rev. D8 (1973) 172.
[120] G.A. Rinker and L. Wilets, Phys. Rev. Letters 34 (1975) 339;
D.H. Fujimoto, Phys. Rev. Letters 35 (1975) 341;
E. Borie, Nucl. Phys. A267 (1976) 485.
[121] H. Fischer, rapporteur's talk; Proc. VIIth Intern. Conf. on High-Energy Physics and Nuclear Structure, Zurich 1977 (Birkhäuser, Basel 1977).
[122] H.L. Anderson et al., Phys. Rev. Letters 38 (1977) 1450; 37 (1976) 4.
[123] C. Jarlskog and H. Pilkuhn, Nucl. Phys. B1 (1967) 264.
[124] S.M. Berman and D.A. Geffen, Nuovo Cim. 18 (1960) 1192.
[125] (a) S. Devons and J. Duerdoth, Advanc. Nucl. Phys. 2 (1969) 295.
(b) C.S. Wu and L. Wilets, Ann. Rev. Nucl. Sci. 19 (1969) 529.
[126] R. Engfer et al., Atomic and Nuclear Data Tables 14 (1974) 509.
[127] H.J. Pfeiffer, K. Springer and H. Daniel, Nucl. Phys. A254 (1975) 433;
H.J. Pfeiffer and H. Daniel, Z. Physik A275 (1975) 313, and references quoted therein.
[128] W. Dey, thesis No. 5473, ETH Zurich (1975);
W. Dey et al., to be published.
[129] D. McLoughlin et al., Phys. Rev. C13 (1976) 1644.
[130] R.J. Powers et al., Nucl. Phys. A278 (1977) 477.
[131] H. Kopfermann, Kernmomente (Akad. Verlagsgesellschaft, Frankfurt a.M. 1956).
[132] (a) P. Ebersold et al., Phys. Letters 53B (1974) 48.
(b) P. Ebersold et al., Nucl. Phys. to be published.
[133] G.J. Ritter, Phys. Rev. 126 (1962) 240.
[134] V.S. Korolkov and A.G. Makhanek, Opt. Spectry. USSR 12 (1962) 87.
[135] J. Lindgren and A. Rosén, Case Studies in Atomic Physics Vol. 4 (1974) No's 3, 4.
[136] B. Elbek, thesis University of Copenhagen (1963).
[137] F. Scheck, Nucl. Phys. B42 (1972) 573.
[138] "Questo e quel pezzo di calamita, pietra Mesmerica, ch'ebbe l'origine n'ell Allemagna, che poi si celebre la in Francia fu", W.A. Mozart/L. da Ponte, in: Cosi fan tutte (1789/90) scene 16 of 1st act.
[139] Charles Burney, The Present State of Music in France and Italy (London 1771).

RECENT DEVELOPMENTS IN CONFORMAL INVARIANT QUANTUM FIELD THEORY

E.S. FRADKIN

P.N. Lebedev Physical Institute of the USSR Academy of Sciences, Moscow, USSR

and

M.Ya. PALCHIK

Institute of Automation and Electrometry of the USSR Academy of Sciences, Novosibirsk, USSR

NORTH-HOLLAND PUBLISHING COMPANY – AMSTERDAM